

**Volume 4. Catalysis, Heterogeneous Systems, Gas Phase Systems****Section 1: Catalysis of electron transfer****4.1.3 Homogeneous redox catalysis in CO<sub>2</sub> fixation**

Etsuko Fujita and Bruce S. Brunshwig

Chemistry Department, Brookhaven National Laboratory, Upton, NY 11973-5000

**Introduction****1. Macrocyclic complexes of cobalt and nickel****1.1 Overview of CO<sub>2</sub> reduction systems mediated by cobalt and nickel  
macrocycles****1.2 Properties of the cobalt and nickel macrocycles****1.2.1 M(I) complexes****1.2.2 M-H complexes****1.2.3 M-CO<sub>2</sub> complexes****1.3 Electrocatalytic systems****1.4 Photocatalytic systems involving CoHMD and Ni(cyclam) complexes****1.4.1 Systems with Ru(bpy)<sub>3</sub><sup>2+</sup>/Ni(cyclam)<sup>2+</sup>****1.4.2 System with p-terphenyl/CoHMD<sup>2+</sup>****1.4.3 Systems with phenazine/CoHMD<sup>2+</sup>****2. Re( $\alpha$ -diimine)(CO)<sub>3</sub>X, Re( $\alpha$ -diimine)(CO)<sub>2</sub>XX' or similar complexes****2.1 Overview of CO<sub>2</sub> reduction systems mediated rhenium complexes****2.2 Properties of Re( $\alpha$ -diimine)(CO)<sub>3</sub>X and Re( $\alpha$ -diimine)(CO)<sub>2</sub>XX'****2.2.1 Redox properties****2.2.2 Excited-state photochemistry and photophysics****2.2.3 Formate-rhenium complexes****2.2.4 Re-CO<sub>2</sub> and Re-COOH complexes**

**2.3 Electrochemical studies: One-electron and two-electron pathways**

**2.4 Photochemical CO<sub>2</sub> reduction with Re( $\alpha$ -diimine)(CO)<sub>3</sub>X and Re( $\alpha$ -diimine)(CO)<sub>2</sub>XX'**

**3. Conclusions**

**Acknowledgement**

**Appendix: Abbreviations**

**References**

## Introduction

The twin problems of global warming and diminishing finite fossil fuels resources have stimulated research into CO<sub>2</sub> fixation and utilization. Natural photosynthetic CO<sub>2</sub> fixation utilizes sunlight and chlorophyll as the energy source and photocatalyst to generate carbohydrates and oxygen from CO<sub>2</sub> and H<sub>2</sub>O. Natural photosynthesis occurring over a few hundred million years has created a vast quantity of fossil fuels that currently fill our current energy needs. Unfortunately, current consumption rates are rapidly depleting our supply of fossil fuels. Even with the advent of fuel farms it is unlikely that natural photosynthesis will be able to balance the production and use of fuels. It is therefore necessary to explore alternative routes to fuel (and chemical) production and it is likely that artificial photosynthesis will play an increasingly important role in the future.

Because of the thermodynamic stability and chemical inertness of CO<sub>2</sub>, both energy and catalysts are needed to transform CO<sub>2</sub> into fuels or useful chemicals. The large energy input needed to fix CO<sub>2</sub> requires the use of renewable energy if artificial CO<sub>2</sub> fixation is carried out on a large scale. The reduction potential to convert CO<sub>2</sub> to CO<sub>2</sub><sup>-</sup> is -1.9 V vs. NHE, making this process highly unfavorable. In fact 0.1 to 0.6 V overpotentials are typically for the single-electron reduction of CO<sub>2</sub> at Pt or Hg working electrodes. This overvoltage partially results from the kinetic barrier arising from the geometric changes required for one-electron reduction of CO<sub>2</sub> (CO<sub>2</sub> is linear while CO<sub>2</sub><sup>-</sup> is bent). Although CO<sub>2</sub> reduction by the proton-assisted multielectron steps shown Table 1 is often kinetically difficult, these steps are more favorable thermodynamically than the one-electron process.

Table 1. Reduction Potentials for CO<sub>2</sub> at pH = 7 with all other solutes at 1M.

Reaction	$E_{1/2}^{\prime a}$ , V	
$\text{CO}_2 + e^- \rightarrow \text{CO}_2^-$	-1.9	(1)
$\text{CO}_2 + 2\text{H}^+ + 2e^- \rightarrow \text{HCO}_2\text{H}$	-0.61	(2)



<sup>a</sup> Values are for water vs NHE. The  $E_{1/2}'$  values in water vs NHE are close to the values in acetonitrile vs SCE because the ferricenium/ferrocene redox potential shifts by 0.25 V (vs SCE) on going from acetonitrile to water while the SCE potential in water is 0.24 V [1, 2].

Since the two-electron reduction to formic acid or CO requires a lower potential, electrolysis using a multielectron transfer catalyst in aqueous or in low protic media can be carried out at considerably lower voltages. The simplest electrocatalytic system for CO<sub>2</sub> reduction is an electrochemical cell that contains: a working electrode, a reference electrode, a homogeneous electrocatalyst, the supporting electrolyte, CO<sub>2</sub> and an oxidizable species (often the solvent). The electrodes, such as those made of Mg, can be used as the oxidizable species. A heterogeneous catalyst attached to the electrode surface can be used in place of the homogeneous electrocatalyst.

The same considerations apply in the photochemical reduction of CO<sub>2</sub>: the one-electron reduction to CO<sub>2</sub><sup>-</sup> requires extremely strong reducing agents that are generally difficult to produce by photochemical methods utilizing visible light. The prototype photochemical system for CO<sub>2</sub> reduction contains a photosensitizer (or photocatalyst) to capture the photon energy, an electron relay catalyst (that might be the same species as the photosensitizer) to couple the photon energy to the chemical reduction, an oxidizable species to complete the redox cycle, and CO<sub>2</sub> as the substrate. Figure 1 shows a cartoon of the photochemical CO<sub>2</sub> reduction system. An effective photocatalyst must absorb a significant part of the solar spectrum, have a long-lived excited state, and promote the activation of small molecules. Both organic dyes and transition-metal complexes have been used as photocatalysts for CO<sub>2</sub> reduction.

## 1. Macrocyclic complexes of cobalt and nickel

### 1.1 Overview of CO<sub>2</sub> reduction systems mediated by cobalt and nickel macrocycles

Many 14-membered tetraazamacrocyclic complexes of cobalt and nickel serve as catalysts for electrochemical CO<sub>2</sub> reduction to produce CO and H<sub>2</sub> in water, acetonitrile/water, or organic solvents<sup>[3-6]</sup>. The structures of the macrocycles are shown in Figure 2. Among these, Ni(cyclam)<sup>2+</sup> is a very effective and selective catalyst for the electrochemical reduction of CO<sub>2</sub> to CO<sup>[5, 6]</sup>. Ni(cyclam)<sup>+</sup> adsorbed on the surface of the mercury electrode has been shown to be the active species. Ni(cyclam)<sup>2+</sup> can have at least two isomers in solution (Figure 2) and studies on configurationally pure nickel complexes similar to Ni(cyclam)<sup>+</sup> have been carried out to measure the activity of different isomers<sup>[7]</sup>. Structural differences are an important factor for both CO<sub>2</sub> binding and catalyst adsorption on mercury.

CoHMD<sup>2+</sup> homogeneously catalyzes both electroreduction of CO<sub>2</sub> and water reduction in water, water/acetonitrile, or DMF solutions<sup>[3, 4]</sup>. The CO-to-H<sub>2</sub> ratio produced is typically less than 1 and strongly depends on the experimental conditions used (i.e., applied potential, amount of water, electrolysis time, etc). The chiral N-H centers of the HMD macrocycle give rise to two isomers, N-rac and N-meso as shown in Figure 2. The N-rac isomers of both Co<sup>II</sup>HMD<sup>2+</sup> and Co<sup>I</sup>HMD<sup>+</sup> predominate in MeCN (>90 %) and water at room temperature. The equilibrium between the N-rac and N-meso cobalt(II) isomers is very slowly established in acidic aqueous and organic media (< 2 × 10<sup>-7</sup> s<sup>-1</sup>); by contrast, equilibration of the cobalt(I) isomers is relatively rapid (> 2 × 10<sup>3</sup> s<sup>-1</sup>)<sup>[8, 9]</sup>.

Photochemical CO<sub>2</sub> reduction to CO (and formate in some cases) has been reported in a catalytic system using Ru(bpy)<sub>3</sub><sup>2+</sup> as the sensitizer, nickel or cobalt macrocycles as the electron relay catalyst, and ascorbate as a sacrificial reductive quencher<sup>[4, 10, 11]</sup>. These systems also produce H<sub>2</sub> via water reduction. While Ni(cyclam)<sup>2+</sup> is an efficient and selective catalyst for electrochemical CO<sub>2</sub> reduction, even in H<sub>2</sub>O, when used as a homogenous catalyst the quantum

yield and selectivity for CO formation is low. The yields of CO and H<sub>2</sub> are pH dependent and typically more H<sub>2</sub> than CO is produced.

Photoreduction of CO<sub>2</sub> with *p*-terphenyl (TP) as the photosensitizer and a tertiary amine as a sacrificial electron donor has been demonstrated[12]. The same system with the addition of a cobalt macrocycle enhances the activity of the TP by suppressing degradative reactions of the TP and produces CO and formate efficiently with only small amounts of H<sub>2</sub>.

Metal(I), metal(III) hydride, and metallocarboxylate complexes have all been postulated as intermediates in electro- and/or photo-chemical CO<sub>2</sub> reduction. These intermediates are discussed in the next sections.

## 1.2. Properties of the cobalt and nickel macrocycles

### 1.2.1 M(I) complexes

Reduction potentials of Ni<sup>II</sup>(cyclam)<sup>2+</sup>, *RRSS*-Ni<sup>II</sup>HTIM<sup>2+</sup> and Co<sup>II</sup>HMD<sup>2+</sup> are -1.44, -1.43, -1.34 V (vs SCE in MeCN), respectively. The metal(I) complexes can be prepared by electrochemical, Na-Hg reduction, or pulse radiolysis. The spectra of all the M(I) species show a strong MLCT (metal-to-ligand charge transfer) band in the visible region ( $\lambda_{\text{max}}$ ,  $\epsilon$ ): Ni<sup>I</sup>(cyclam)<sup>+</sup> at 384 nm, 4400 M<sup>-1</sup> cm<sup>-1</sup>; *RRSS*-Ni<sup>I</sup>HTIM<sup>+</sup> at 388 nm, 4340 M<sup>-1</sup> cm<sup>-1</sup>; and Co<sup>I</sup>HMD<sup>+</sup> at 678 nm, 18,000 M<sup>-1</sup> cm<sup>-1</sup> in MeCN. In the square-planar d<sup>8</sup>-Co<sup>I</sup>HMD<sup>+</sup>, the electron-rich cobalt(I) center donates significant electron density to the imine moiety, causing the C=N stretching frequency (1571 cm<sup>-1</sup>) to be much lower than for Co<sup>II</sup>HMD<sup>2+</sup> (1661 cm<sup>-1</sup>). Interestingly, the square-planar d<sup>9</sup>-NiHMD<sup>+</sup> complex donates less electron density: the C=N stretching frequency only shifts from 1655 to 1647 cm<sup>-1</sup> upon the reduction ( $E_{1/2} = -1.22$  V vs SCE in MeCN). EXAFS and x-ray structures reveal that the Co-N bond distances remain almost the same upon the reduction of the Co(II) macrocycles in both solid and solution[13, 14].

Square-planar d<sup>8</sup>-Ni(cyclam)(ClO<sub>4</sub>)<sub>2</sub> and *RRSS*-NiHTIM(ClO<sub>4</sub>)<sub>2</sub> can be crystallized from water as low spin complexes. However, in solution the Ni(III) complexes can exist as high spin, octahedral complexes and/or as low spin, square-planar complexes depending on solvent[15].

For example,  $\text{Ni}^{\text{II}}(\text{cyclam})^{2+}$  and  $\text{Ni}^{\text{II}}\text{HTIM}^{2+}$  are low spin in  $\text{MeNO}_2$ , high spin in  $\text{MeCN}$ , and the high and low spin complexes are in equilibrium in water. EXAFS studies reveal that *RRSS*- $\text{Ni}^{\text{II}}\text{HTIM}^{2+}$  and *RRSS*- $\text{Ni}^{\text{I}}\text{HTIM}^+$  are 6-coordinate and 4-coordinate with avg. Ni-N distances of 2.08 Å and 2.05 Å, respectively, in  $\text{MeCN}$ [16]. The x-ray structures of square-planar *RSSR*- $\text{Ni}^{\text{II}}\text{HTIM}(\text{ClO}_4)_2$  (avg. Ni-N distance: 1.959 Å) and *RSSR*- $\text{Ni}^{\text{I}}\text{HTIM}(\text{ClO}_4)$  (avg. Ni-N distance: 2.068 Å) indicate that the bond lengths in the Ni(I) macrocycles increase 0.11 Å upon reduction[15]. This suggests that the  $\text{Ni}^{\text{II/I}}$  self-exchange rates of both  $\text{Ni}(\text{cyclam})$  and *RSSR*- $\text{NiHTIM}$  complexes in  $\text{MeCN}$  will be slow due to the large structural changes upon electron transfer.

Some electron-transfer rates are summarized in Table 2. Owing to the large driving force for most of the reactions ( $> 1.1 \text{ V}$ ), the rates constants are mostly  $> 10^{10} \text{ M}^{-1} \text{ s}^{-1}$  and are at or near the diffusion controlled limit. It would be helpful to have firm determinations of the self-exchange rates constants for the nickel systems.

Table 2. Comparison of electron transfer rates at 25 °C<sup>a</sup>

Reaction	Complex	k, M <sup>-1</sup> s <sup>-1</sup>	Ref.
ML <sup>2+</sup> + e <sup>-</sup> <sub>aq</sub> → ML <sup>+</sup>	Ni(cyclam) <sup>2+</sup>	5.6 × 10 <sup>10</sup>	[17]
	Ni(cyclam) <sup>2+</sup>	4.1 × 10 <sup>10</sup>	[18]
	RSSR-NiHTIM <sup>2+</sup>	3.5 × 10 <sup>10</sup>	[19]
	<i>N-rac</i> -CoHMD <sup>2+</sup>	4.4 × 10 <sup>10</sup>	[20]
	<i>N-meso</i> -CoHMD <sup>2+</sup>	4.7 × 10 <sup>10</sup>	[9]
ML <sup>2+</sup> + TP <sup>•-</sup> → ML <sup>+</sup> + TP	Ni(cyclam) <sup>2+</sup>	4.3 × 10 <sup>9</sup>	[21]
	<i>N-rac</i> -CoHMD <sup>2+</sup>	1.1 × 10 <sup>10</sup>	[22]
	CoOMD <sup>2+</sup>	1.1 × 10 <sup>10</sup>	[22]
	CoDMD <sup>2+</sup>	8.8 × 10 <sup>9</sup>	[22]
ML <sup>2+</sup> + Ru(bpy) <sub>3</sub> <sup>+</sup> → ML <sup>+</sup> + Ru(bpy) <sub>3</sub> <sup>2+</sup>	<i>N-rac</i> -CoHMD <sup>2+</sup>	1.8 × 10 <sup>8</sup>	[23]
	Ni(cyclam) <sup>2+</sup>	Never reported	

<sup>a</sup> The reaction rates with e<sup>-</sup><sub>aq</sub> are measured in water. The electron-transfer rate from TP<sup>•-</sup>, which has a potential estimated at about -2.5 V, is measured in MeCN. The electron-transfer rate from Ru(bpy)<sub>3</sub><sup>+</sup>, which has a potential of -1.33 V, is measured in H<sub>2</sub>O.

### 1.2.2 M-H complexes

Although both cobalt(I) and nickel(I) macrocycles are stable in dry degassed MeCN, their lifetimes in water are limited because the M(I) complexes react with protons to form the corresponding metal hydrides, M(III)-H, as shown in Eq. 8.



The thermodynamics and kinetics of  $H^+$  binding to cobalt(I) and nickel(I) macrocycles have been determined. The  $pK_a$  of  $Ni(cyclam)(H)^{2+}$ ,  $RRSS-NiHTIM(H)^{2+}$ , and  $N-rac-CoHMD(H)^{2+}$  are 1.8, 1.9, and 11.7, respectively[9, 18, 21]. As seen from Table 3, protonation rate constants for  $N-rac-CoHMD^+$  depend on acid strength. The results are consistent with an associative reaction of the square-planar complex with an acid, HA. While the spectrum of  $N-rac-CoHMD(H)^{2+}$  suggests the formation of a  $[Co^{III}(H^-)]^{2+}$  species with an absorption band at 440 nm ( $520 M^{-1} cm^{-1}$ ),  $Ni(cyclam)(H)^{2+}$  shows no significant absorbance in the 300-700 nm region[9, 18].

Table 3. Rate constants for protonation of  $M(I)L^+$  by acid (HA)

Complex	HA	$pK_a$ of HA	I, M	$k, M^{-1}s^{-1}$	Ref.
$N-rac-Co^I HMD^+$	$H_3O^+$	-1.75	0.015	$3.1 \times 10^9$	[20]
	HCOOH	3.5	0.02	$1.7 \times 10^8$	[9]
	MeCOOH	4.5	0.1	$1.1 \times 10^8$	[9]
	MeCOOH	4.5	0.1	$0.75 \times 10^8$	[20]
	$H_2PO_4^-$	6.5	0.1	$0.8 \times 10^8$	[9]
	$H_2PO_4^-$	6.5	0.1	$0.98 \times 10^8$	[20]
	$H_2PO_4^-$	6.5	0.008	$1.2 \times 10^8$	[9]
	$HCO_3^-$	10.3	0.1	$2.5 \times 10^6$	[9]
	$H_3BO_3$	9.3	0.1	$0.7 \times 10^5$	[9]

	HPO <sub>4</sub> <sup>2-</sup>	12.25	0.2	1 × 10 <sup>5</sup>	[20]
<i>N-meso</i> -Co <sup>I</sup> HMD <sup>+</sup>	H <sub>3</sub> O <sup>+</sup>	-1.75	0.015	2.3 × 10 <sup>9</sup>	[9]
	HCOOH	3.5	0.02	1.8 × 10 <sup>8</sup>	[9]
	MeCOOH	4.5	0.1	0.8 × 10 <sup>8</sup>	[9]
Ni <sup>I</sup> (cyclam) <sup>+</sup>	H <sub>2</sub> PO <sub>4</sub> <sup>-</sup>	6.5	0.1	1.2 × 10 <sup>8</sup>	[9]
	H <sub>3</sub> O <sup>+</sup>	-1.75	0.06-	1.1 × 10 <sup>5</sup>	[17]
			0.3		
	H <sub>3</sub> O <sup>+</sup>	-1.75	0.006	3 × 10 <sup>7</sup>	[18]
	MeCOOH	4.5	0.015-	1.2 × 10 <sup>4</sup>	[17]
			0.3		
	H <sub>2</sub> PO <sub>4</sub> <sup>-</sup>	6.5	0.01-	< 10 <sup>4</sup>	[17]
			0.1		

### 1.2.3 M-CO<sub>2</sub> complexes

The reversible binding of CO<sub>2</sub> to M<sup>I</sup>L<sup>+</sup> has been studied using differential pulse polarography[24], cyclic voltammogram[25, 26], pulse radiolysis[9, 18], flash photolysis[18, 22], and conventional spectroscopic methods[26, 27]. The results are summarized in Table 4. The CO<sub>2</sub> binding constants of *N-meso*- and *N-rac*-Co<sup>I</sup>HMD<sup>+</sup> are quite different in both H<sub>2</sub>O and MeCN.



The CO<sub>2</sub> binding constant for the *N-rac* isomer is about one-hundred times greater than for the *N-meso* isomer in both solvents. The difference is primarily due to steric interactions between the bound CO<sub>2</sub> and the macrocycle. While hydrogen bonding between the bound CO<sub>2</sub> and amine protons of the macrocycle stabilizes both adducts, the *N-meso* adduct is destabilized by steric repulsion between the macrocycle methyl groups and the CO<sub>2</sub>. The equilibrium constants for the formation of CoHMD(CO<sub>2</sub>)<sup>+</sup> and Ni(cyclam)(CO<sub>2</sub>)<sup>+</sup> are ≈ 10<sup>4</sup> and 4 times larger in water than in

MeCN, respectively. Water may stabilize the CoHMD(CO<sub>2</sub>) complex by forming hydrogen bonds to the bound CO<sub>2</sub> as found in crystals of [Ru(bpy)<sub>2</sub>(CO)(COO)]•3H<sub>2</sub>O[28]. However, both CoHMD(CO<sub>2</sub>)<sup>+</sup> and Ni(cyclam)(CO<sub>2</sub>)<sup>+</sup> have shorter lifetimes in water than in MeCN due to subsequent reactions.

A redox potential threshold for CO<sub>2</sub> binding to the cobalt macrocycles seems to occur at ~ -1.2 V vs SCE[26]. The CO<sub>2</sub> binding constants for a series of Co(I) macrocycles show a strong correlation with the Co<sup>II/I</sup> potential. This trend is consistent with charge transfer from the electron-rich cobalt center to the bound CO<sub>2</sub>. The CO<sub>2</sub> binding rate constants seem also to correlate with the Co<sup>II/I</sup> potential:  $1.1 \times 10^6 \text{ M}^{-1} \text{ s}^{-1}$  for Co<sup>I</sup>OMD<sup>+</sup>,  $1.7 \times 10^8 \text{ M}^{-1} \text{ s}^{-1}$  for Co<sup>I</sup>HMD<sup>+</sup> and  $3.7 \times 10^8 \text{ M}^{-1} \text{ s}^{-1}$  for Co<sup>I</sup>DMD<sup>+</sup>.

Table 4. Equilibrium and Rate Constants for the Reaction of  $ML^+$  with  $CO_2$  in various solvents<sup>a</sup>

Complex	Solvent	$E_{1/2}$ , V	$K_{CO_2}$ , $M^{-1}$	$k_f$ , $M^{-1}s^{-1}$	$k_r$ , $s^{-1}$	Ref
$Co^I HMD^+$	DMSO	-1.29 <sup>b</sup>	$7 \times 10^4$			[24]
<i>N-rac</i> - $Co^I HMD^+$	DMSO	-1.74 <sup>c</sup>	$3.0 \times 10^4$			[25]
	Propylene carbonate	-1.54 <sup>c</sup>	$4.0 \times 10^4$			[25]
	DMF	-1.77 <sup>c</sup>	$1.8 \times 10^4$			[25]
	THF	-1.77 <sup>c</sup>	$3.0 \times 10^3$			[25]
	H <sub>2</sub> O	irr	$2.5 \times 10^8$	$1.7 \times 10^8$	(0.38)	[9]
	MeCN <sup>d</sup>	-1.34 <sup>b</sup>	$1.2 \times 10^4$	$1.8 \times 10^8$	$(1.5 \times 10^4)$	[26, 27]
	MeCN	-1.34 <sup>b</sup>	$1.4 \times 10^4$	$1.8 \times 10^8$	$(1.3 \times 10^4)$	[22]
	MeCN/MeOH		$1.1 \times 10^4$	$1.7 \times 10^8$	$3 \times 10^4$	[22]
<i>N-meso</i> - $Co^I HMD^+$	DMSO	-1.74 <sup>c</sup>	260			[25]
	MeCN	-1.34 <sup>b</sup>	170			[26]
	H <sub>2</sub> O	irr	$6.0 \times 10^6$	$1.5 \times 10^7$	2.7	[9]
$Co^I OMD^+$	MeCN/MeOH		6	$1.1 \times 10^6$	$1.8 \times 10^5$	[22]
	MeCN	-1.28 <sup>b</sup>	4			[29]
$Co^I DMD^+$	MeCN/MeOH		$> 5 \times 10^4$	$3.7 \times 10^8$	$(< 7 \times 10^8)$	[22]

	MeCN	-1.51 <sup>b</sup>	$7 \times 10^5$	[29]
Ni <sup>I</sup> (cyclam) <sup>+</sup>	MeCN	-1.44 <sup>b</sup>	4	[7, 15]
	H <sub>2</sub> O	-1.52 <sup>b</sup>	16	[18]
RRSS-Ni <sup>I</sup> HTIM <sup>+</sup>	MeCN	-1.43 <sup>b</sup>	$(3.2 \times 10^7)$	$2.0 \times 10^6$
				[7, 15]

<sup>a</sup> Numbers in parentheses are calculated values. <sup>b</sup> Measured vs SCE <sup>c</sup> Measured vs ferricinium/ferrocene <sup>d</sup> The  $K_{\text{CO}_2}$  is assumed to be the same as  $K_9$  in Eq. 9.

Although the *N-rac*-CoHMD(CO<sub>2</sub>)<sup>+</sup> adduct decomposes to *N-rac*-CoHMD<sup>2+</sup> and CO in wet MeCN, it is stable in dry MeCN under a CO<sub>2</sub> atmosphere. The complex is thermochromic, being purple at room temperature and yellow at low temperature[29]. The 530-nm band diminishes in intensity and a 430-nm band increases in intensity as the temperature drops. Measurements over the range -40 to +40 °C give  $K_s(298) = 0.11 \pm 0.13$ ,  $\Delta G^\circ(298) \approx 1.3$  kcal mol<sup>-1</sup>,  $\Delta H^\circ = -7.0$  kcal mol<sup>-1</sup> and  $\Delta S^\circ = -28$  cal K<sup>-1</sup> mol<sup>-1</sup> for Eq. 11 in MeCN.



A solid sample, obtained at -70 °C from a THF/MeCN mixture, shows  $\nu_{\text{C=O}} = 1558$  cm<sup>-1</sup>,  $\nu_{\text{C=N}} = 1653$  cm<sup>-1</sup>, and two  $\nu_{\text{C=N}}$ , 2337 cm<sup>-1</sup> (for coordinated MeCN) and 2272 cm<sup>-1</sup> (for free MeCN), consistent with the formation of [S-CoHMD(CO<sub>2</sub>)]<sup>+</sup> with S = MeCN. Increasing pressure also causes the color to change. A MeCN solution contains ~80% five-coordinate [CoHMD(CO<sub>2</sub>)]<sup>+</sup> and ~20% six-coordinate [CoHMD(CO<sub>2</sub>)(MeCN)]<sup>+</sup> under atmospheric pressure at 15° C. Increasing pressure shifts the equilibrium toward the six-coordinate species with an overall reaction volume  $\Delta V^\circ = -17.7$  mL mol<sup>-1</sup>[30]. Furthermore, the FTIR spectra measured over the range 25 to -75 °C in a CD<sub>3</sub>CN/THF mixture indicate the existence of four CO<sub>2</sub> adducts: a five-coordinate, non-hydrogen-bonded form **A** ( $\nu_{\text{C=O}} = 1710$  cm<sup>-1</sup>,  $\nu_{\text{NH}} = 3208$  cm<sup>-1</sup>), a five-coordinate intramolecular hydrogen-bonded form **B** ( $\nu_{\text{C=O}} = 1626$  cm<sup>-1</sup>), a six-coordinate non-hydrogen bonded form **C** ( $\nu_{\text{C=O}} = 1609$  cm<sup>-1</sup>,  $\nu_{\text{NH}} = 3224$  cm<sup>-1</sup>), and a six-coordinate intramolecular hydrogen-bonded form **D** ( $\nu_{\text{C=O}} = 1544$  cm<sup>-1</sup>,  $\nu_{\text{NH}} = 3145$  cm<sup>-1</sup>). (See Figure 3.) The two five-coordinated (A and B) and two six-coordinated (C and D) species have similar UV-vis spectra, so only two species are observed by UV-vis spectroscopy.

The thermochromic behavior of the CO<sub>2</sub> adducts has been studied by an X-ray absorption spectroscopy[14]. The metal coordination number, geometry, and electronic properties can be studied using X-ray absorption near-edge spectroscopy while metal-ligand bond distances can be obtained through analysis of the extended X-ray absorption fine structure. XANES spectra for a series of the CoHMD complexes are shown in Figure 4. The X-ray absorption edge position of

the CoHMD complex is sensitive to the oxidation state of the cobalt. The edge energy of  $\text{Co}^{\text{II}}\text{HMD}^{2+}$  decreases (1 eV) upon reduction and increases (2-eV) upon oxidation as can be seen in Figure 4a. The  $1s \rightarrow 4p_z$  pre-edge peak, located  $\approx 6$  eV below the main edge, in the XANES spectrum for  $\text{Co}^{\text{II}}\text{HMD}^{2+}$  is characteristic of a four-coordinate square-planar geometry. The XANES spectra of the  $\text{CO}_2$  adducts at room temperature and 150 K are shown in Figure 4b. At room temperature the Co- $\text{CO}_2$  adduct is 90% five-coordinate  $\text{CoHMD}(\text{CO}_2)^+$  and 10% six-coordinate S- $\text{CoHMD}(\text{CO}_2)^+$ , whereas cooling the solution to 150 K results in 100% conversion to the six-coordinate species<sup>[26]</sup>. The edge position of  $\text{CoHMD}(\text{CO}_2)^+$  at room temperature is similar to that of  $\text{Co}^{\text{II}}\text{HMD}^{2+}$ , consistent with theoretical predictions<sup>[31, 32]</sup> that the bound  $\text{CO}_2$  receives significant electrons density ( $\approx 0.7$  of an electron) mainly from the Co  $d_z^2$  orbital. The XANES spectrum for S- $\text{CoHMD}(\text{CO}_2)^+$  at 150 K shows an increase of the  $1s \rightarrow 3d$  peak ( $\approx 11$  eV below the main edge) and almost complete loss of the  $1s \rightarrow 4p_z$  transitions, indicative of six-coordinate distorted octahedral geometry. The six-coordinate S- $\text{CoHMD}(\text{CO}_2)^+$  species shows a 1.2 eV shift towards Co(III) and is interpreted as a  $\text{Co}^{\text{III}}\text{-CO}_2^{2-}$  carboxylate complex. This assignment is consistent with the change of the  $\text{CO}_2$  asymmetric stretch,  $\nu_{\text{C=O}}$ , from  $1710 \text{ cm}^{-1}$  for  $\text{CoHMD}(\text{CO}_2)^+$  to  $1544 \text{ cm}^{-1}$  for S- $\text{CoHMD}(\text{CO}_2^{2-})^+$  discussed above. Although the cobalt(III) carboxylates have been postulated as intermediates in  $\text{CO}_2$  reduction and water-gas shift reactions, the XANES results provide the first unambiguous evidence that active metal catalysts, such as  $\text{Co}^{\text{I}}\text{HMD}^+$ , can promote two-electron transfer to the bound  $\text{CO}_2$ . The conversion of the  $\text{M}^{\text{I}}\text{CO}_2$  species to a metallocarboxalate,  $\text{M}^{\text{III}}(\text{CO}_2^{2-})$ , is an important step in catalytic  $\text{CO}_2$  reduction since it avoids the very high energy  $\text{CO}_2^-$  species.

### 1.3 Electrocatalytic systems

$\text{Ni}(\text{cyclam})^{2+}$  is a very effective and selective catalyst for the electrochemical reduction of  $\text{CO}_2$ <sup>[5, 6]</sup>. The advantages of the catalyst are: high turnover frequencies (up to  $10^3$  cycles  $\text{h}^{-1}$ ); accessibility of the applied potential; high efficiency; good selectivity of CO formation at pH 4; and stability of the catalyst after a large number of turnovers ( $> 10^4$ ).  $\text{Ni}(\text{cyclam})^+$  adsorbs on the

surface of the mercury electrode and the adsorbed complex is the active catalyst.  $\text{Ni}(\text{cyclam})^{2+}$  has configurational isomers in solution; the most stable two forms (*Trans III*, 85 % and *Trans I*, 14 % in water) are shown in Figure 2. It is possible to lock the cyclam ligand in one configuration (*Trans III*) by adding methyl groups to the six-membered ring as in HTIM. The catalytic activities of pure stereo-isomers, *RRSS*- and *RSSR*- $\text{NiHTIM}^{2+}$  have been studied[7]. These isomers do not show any isomerization in solution. *RRSS*- $\text{NiHTIM}^{2+}$ , which has no axial methyl groups, shows much higher catalytic activity than *RSSR*- $\text{NiHTIM}^{2+}$ . *RRSS*- $\text{NiHTIM}^{2+}$  has larger catalytic currents and more positive potentials for  $\text{CO}_2$  reduction than  $\text{Ni}(\text{cyclam})^{2+}$ . The peak current density of the *RSSR*- $\text{NiHTIM}^{2+}$ , which has axial methyl groups, is lower than that of  $\text{Ni}(\text{cyclam})^{2+}$ [7]. Thus structural differences may play an important role in adsorption of the metal complex on a mercury electrode and in  $\text{CO}_2$  binding by the adsorbed complex.

$\text{CoHMD}^{2+}$  homogeneously catalyzes electroreduction of  $\text{CO}_2$ . However, it also catalyzes water reduction in water, water/acetonitrile, and DMF solutions[3, 4]. The  $\text{CO}$ -to- $\text{H}_2$  ratio strongly depends on the experimental conditions used (i.e., applied potential, amount of water, electrolysis time, etc) and is typically less than 1. Since the  $\text{pK}_a$  of  $\text{CoHMD}(\text{H})^{2+}$  is 11.7, the hydride species also form in  $\text{CO}_2$ -saturated water ( $\text{pH} \sim 4$ )[3, 4].

#### 1.4. Photocatalytic systems involving CoHMD and Ni(cyclam) complexes

##### 1.4.1 Systems with $\text{Ru}(\text{bpy})_3^{2+}/\text{Ni}(\text{cyclam})^{2+}$

$\text{CO}_2$  can be reduced using photogenerated reductants as shown in Figure 1. Photochemical  $\text{CO}_2$  reduction has been reported in a catalytic system using  $\text{Ru}(\text{bpy})_3^{2+}$  as the sensitizer,  $\text{Ni}(\text{cyclam})^{2+}$  as the electron relay catalysts and ascorbate as a sacrificial reductive quencher (Table 5)[10, 11]. The quantum yield for  $\text{CO}$  production is  $\sim 10^{-4}$  at  $\text{pH} = 4$  with low selectivity for  $\text{CO}$  formation due to coproduction of  $\text{H}_2$ . The yield of both  $\text{CO}$  and  $\text{H}_2$  are  $\text{pH}$  dependent. Without  $\text{Ni}(\text{cyclam})^{2+}$ , a system containing  $\text{Ru}(\text{bpy})_3^{2+}$  and TEOA produces  $\text{HCOO}^-$  with a quantum yield  $\sim 5\%$ , but no  $\text{CO}$ [33, 34]. In order to improve the  $\text{CO}$  yield, complexes that covalently link the sensitizer to the catalysts have been prepared. Complexes in which

$\text{Ru}(\text{bpy})_3^{2+}$  or  $\text{Ru}(\text{phen})_3^{2+}$  are bound to  $\text{Ni}(\text{cyclam})^{2+}$  have been studied[35-38]. However, these supramolecular photochemical systems have low yields of CO due to competing processes in the quenching of the photoexcited complexes[35, 38].

Bismacrocylic nickel complexes  $[\text{Ni}_2(\text{bcyclam})]^{4+}$  and  $[\text{Ni}_2(\text{bMe}_2\text{cyclam})]^{4+}$  have been prepared and tested as  $\text{CO}_2$  reduction catalysts. The ligands *bcyclam* and *bMe<sub>2</sub>cyclam* have two connected *cyclam* or *dimethylcyclam* units, respectively, as shown in Figure 2. While  $[\text{Ni}_2(\text{bMe}_2\text{cyclam})]^{4+}$  shows good selectivity and a high yield for CO formation,  $[\text{Ni}_2(\text{bcyclam})]^{4+}$  and the corresponding monomeric nickel complexes ( $\text{Ni}(\text{cyclam})^{2+}$  and  $\text{Ni}(\text{Me}_2\text{cyclam})^{2+}$ ) do not[39]. The authors attribute this to the configuration of the methyl groups which occupy the axial positions of the six-membered chelate rings. However, why axial methyl groups increase the catalytic activity is not clear, since axial methyl groups normally hinder  $\text{CO}_2$  binding.

Table 5. Photochemical CO<sub>2</sub> reduction with metal macrocycles

Sensitizer	Catalyst or Relay	Donor	Product(s)	CO/H <sub>2</sub>	$\Phi^a$ mol einstein <sup>-1</sup>	Ref.
Ru(bpy) <sub>3</sub> <sup>2+</sup>		TEOA	HCOO <sup>-</sup>		0.049 <sup>b</sup>	[33]
						[34]
Ru(bpy) <sub>3</sub> <sup>2+</sup>		TEOA	HCOO <sup>-</sup>		0.096 <sup>c</sup>	[34]
Ru(bpy) <sub>3</sub> <sup>2+</sup>	CoHMD <sup>2+</sup>	H <sub>2</sub> A	CO, H <sub>2</sub>			[4]
Ru(bpy) <sub>3</sub> <sup>2+</sup>	Ni(cyclam) <sup>2+</sup>	H <sub>2</sub> A	CO, H <sub>2</sub>	0.16	0.001 (CO)	[10, 11]
Ru(bpy) <sub>3</sub> <sup>2+</sup>	Ni(cyclam) <sup>2+</sup>	H <sub>2</sub> A	CO, H <sub>2</sub>	0.12		[40]
Ru(bpy) <sub>3</sub> <sup>2+</sup>	Ni(cyclam) <sup>2+</sup>	H <sub>2</sub> A	CO, H <sub>2</sub>	0.4		[39]
Ru(bpy) <sub>3</sub> <sup>2+</sup>	Ni(cyclam) <sup>2+</sup>	H <sub>2</sub> A	CO, H <sub>2</sub>	0.02-0.07		[37]
Ru(bpy) <sub>3</sub> <sup>2+</sup>	Ni(Pr-cyclam) <sup>2+</sup>	H <sub>2</sub> A	CO, H <sub>2</sub>	0.10-0.65	~0.005 <sup>d</sup> (CO)	[37]
Ru(bpy) <sub>3</sub> <sup>2+</sup>	[Ni <sub>2</sub> (bcyclam)] <sup>4+</sup>	H <sub>2</sub> A	CO, H <sub>2</sub>		~0.0006 <sup>d</sup> (CO)	[39]
Ru(bpy) <sub>3</sub> <sup>2+</sup>	[Ni <sub>2</sub> (bMe <sub>2</sub> cyclam)] <sup>4+</sup>	H <sub>2</sub> A	CO, H <sub>2</sub>	15	~0.008 <sup>d</sup> (CO)	[39]
<i>p</i> -Terphenyl	Co(cyclam) <sup>3+</sup>	TEOA	CO, HCOO <sup>-</sup> , H <sub>2</sub>	6	0.075 (HCOO <sup>-</sup> ) 0.05 (CO)	[12, 41]
<i>p</i> -Terphenyl	CoHMD <sup>2+</sup>	TEOA	CO, HCOO <sup>-</sup> , H <sub>2</sub>	1.4		[12]
Phenazine	Co(cyclam) <sup>3+</sup>	TEOA	HCOO <sup>-</sup>		0.035	[42]

<sup>a</sup> Unless otherwise noted, the quantum yield of product formation is defined as the formation rate divided by the light intensity. <sup>b</sup> with 15 % water in DMF. <sup>c</sup> with 15 % water and excess bpy in DMF. <sup>d</sup> Assuming  $\Phi$  for Ni(cyclam)<sup>2+</sup> is 0.001.

### 1.4.2 System with *p*-terphenyl/CoL<sup>2+</sup>

Oligo(*p*-phenylene)s ranging from *p*-terphenyl (TP) to *p*-sexiphenyl sensitize the photoreduction of CO<sub>2</sub> to formic acid. The systems use triethylamine as a sacrificial electron donor in aprotic polar solvents such as DMF and MeCN<sup>[43, 44]</sup>. The photoreduction of CO<sub>2</sub> proceeds via electron transfer from the photogenerated anion radical of the *p*-phenylene directly to the CO<sub>2</sub> molecule. In the case of TP, the quantum yield of HCO<sub>2</sub><sup>-</sup> formation is 3.6% at 313 nm. Unfortunately, a photo-Birch reduction of the TP producing dihydroterphenyl derivatives occurs in parallel with the photoreduction process and the photoactivity is quickly lost. The photodegradation is suppressed when metal macrocycles are added as electron mediators between the reduced terphenyl anion radical and the CO<sub>2</sub>. Thus cobalt macrocycles mediate the photoreduction of CO<sub>2</sub> with TP and a tertiary amine (including the β-hydroxylated tertiary amine) as sacrificial electron donor in acetonitrile/methanol mixtures<sup>[12]</sup>. The system produces CO and formate efficiently with only small amounts of H<sub>2</sub>. The combined quantum yield of CO and formate is 13% at 313 nm in the presence of triethanolamine and Co(cyclam)<sup>3+</sup>.

Mechanistic and kinetic studies of the TEA/TP/CoHMD<sup>2+</sup>/CO<sub>2</sub> system have been investigated<sup>[22]</sup> using flash photolysis techniques. In the absence of added CoHMD<sup>2+</sup> and CO<sub>2</sub>, the TP<sup>•-</sup> spectrum was obtained in MeCN/MeOH within the resolution of the spectrometer, consistent with the reported rate constant for Eq 12 of  $3 \times 10^9 \text{ M}^{-1} \text{ s}^{-1}$  in THF<sup>[44]</sup>; decay of TP<sup>•-</sup> in MeCN/MeOH solution followed first-order kinetics with a rate constant of  $400 \text{ s}^{-1}$ .



The transient absorption spectrum of a sample with added Co<sup>II</sup>HMD<sup>2+</sup> indicates the formation of the reduced cobalt complex, Co<sup>I</sup>HMD<sup>+</sup> (Eq 13)<sup>[27, 29, 45]</sup>. The cobalt(I) complex is quite stable with a lifetime of > 1 s under the experimental conditions (Fig. 6a). The decay of the TP<sup>•-</sup> absorption and the growth of the Co<sup>I</sup>HMD<sup>+</sup> absorption are shown in Figure 6b and 6c, respectively. The observed rate for the decay of TP<sup>•-</sup> and growth of Co<sup>I</sup>HMD<sup>+</sup> are the same. The

magnitudes of the changes in absorbance at 470 and 685 nm establish that the stoichiometry of the formation of Co(I) from TP<sup>•+</sup> is 1 : 1 ± 0.2. A plot of the observed first-order rate constant ( $k_{\text{obsd}}$ ) for the decay of TP<sup>•+</sup> is linear in [Co<sup>II</sup>HMD<sup>2+</sup>] and gives a second-order rate constant close to diffusion controlled as expected due to of the reaction's large driving force (~ 1.1 V).

The dependence of the decay rate of TP<sup>•+</sup> on [CO<sub>2</sub>], measured for solutions containing CO<sub>2</sub> with no cobalt macrocycle is not linear in CO<sub>2</sub> concentration. A rate constant of < 10<sup>6</sup> M<sup>-1</sup> s<sup>-1</sup> is estimated for the TP<sup>•+</sup>/CO<sub>2</sub> reaction. This sluggish rate constant is consistent with the large reorganization of the CO<sub>2</sub>/CO<sub>2</sub><sup>-</sup> couple and modest driving force for the reaction (0.5 V). Under photocatalytic conditions (continuous photolysis) the TP<sup>•+</sup> reacts much faster with the cobalt complex than with CO<sub>2</sub> and > 90 % the photochemically generated reducing equivalents are captured by the cobalt macrocycle.

When CO<sub>2</sub> is introduced into the photosystem, the lifetime of the Co<sup>I</sup>HMD<sup>+</sup> changes dramatically. The decay of Co<sup>I</sup>HMD<sup>+</sup> monitored at 670 nm shown in Figure 7 has a rate constant of 6.5 × 10<sup>4</sup> s<sup>-1</sup>. The observed rate constant for Co<sup>I</sup>HMD<sup>+</sup> decay is linearly dependent on CO<sub>2</sub> concentration. The CO<sub>2</sub> binding rate constant (forward reaction in Eq 15) is 1.7 × 10<sup>8</sup> M<sup>-1</sup>s<sup>-1</sup>.



The decay of the Co<sup>I</sup>HMD<sup>+</sup> under a CO<sub>2</sub> atmosphere results in a finite absorbance at long times (Figure 7). In addition, the transient spectra measured at 50, 25, 0, and -25 °C indicate a mixture of the five- and six-coordinate CO<sub>2</sub> adducts, CoHMD(CO<sub>2</sub>)<sup>+</sup> and S-CoHMD(CO<sub>2</sub>)<sup>+</sup>. Since the CO<sub>2</sub> adducts have no significant absorption at 670 nm, the ratio of the total amount of cobalt-CO<sub>2</sub> complex, [Co(CO<sub>2</sub>)], to the unreacted complex, [CoHMD<sup>+</sup>], is given by the ratio of the change in the absorbance at 670 nm, ( $A_{\infty} - A_0$ ), to the final absorbance at 670 nm (Figure 4a). One can define an effective equilibrium constant

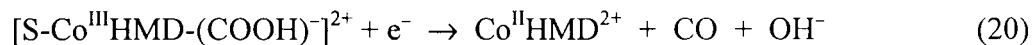
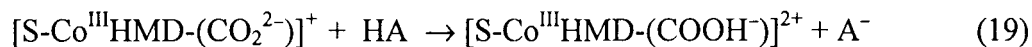
$$\begin{aligned}
K_{\text{CO}_2} &= \frac{[\text{Co}(\text{CO}_2)]_t}{[\text{Co}^{\text{I}}\text{HMD}^+][\text{CO}_2]} \\
&= \frac{A_\infty - A_0}{A_\infty[\text{CO}_2]}
\end{aligned}
\tag{17}$$

where  $[\text{Co}(\text{CO}_2)]_t = [\text{CoHMD}(\text{CO}_2)^+] + [\text{S-CoHMD}(\text{CO}_2)^+]$  and  $A_\infty$  and  $A_0$  are the absorbances at 670 nm at long times and at  $t = 0$ , respectively. The above assumes that the  $\text{Co}^{\text{I}}\text{HMD}^+$  is rapidly formed, both  $\text{Co}^{\text{I}}\text{HMD}^+$  and the  $\text{CO}_2$  adduct are stable on the transient absorption time scale, and only  $\text{Co}^{\text{I}}\text{HMD}^+$  absorbs. When the  $\text{CO}_2$  concentration is lowered,  $(A_\infty - A_0)$  is reduced and  $A_\infty$  increases.  $K_{\text{CO}_2}$  is calculated from Eq 17 as  $1.1 \times 10^4 \text{ M}^{-1}$  as shown in Table 4.

The equilibrium constant  $K_{\text{CO}_2}$  is also given by

$$K_{\text{CO}_2} = K_{15}(1 + K_{16}[\text{S}]) \tag{18}$$

where  $K_{15}$  and  $K_{16}$  are the equilibrium constants for Eq 15 and Eq 16, respectively. Equilibrium studies in MeCN indicates that  $K_{15}$  and  $K_{16}[\text{S}]$  are  $1.2 \times 10^4 \text{ M}^{-1}$  and 0.17, respectively, for  $\text{Co}^{\text{I}}\text{HMD}^+$  at 25 °C [26, 27, 29], yielding a value of  $1.4 \times 10^4 \text{ M}^{-1}$  for the  $K_{\text{CO}_2}$ .  $\text{CO}_2$  binding rate constants determined by transient absorbance in MeCN/MeOH, by cyclic voltammogram in pure MeCN, and by pulse radiolysis in  $\text{H}_2\text{O}$  are all about  $1.7 \times 10^8 \text{ M}^{-1} \text{ s}^{-1}$ . The  $\text{CO}_2$  binding constant obtained by transient methods is in good agreement with the value obtained from equilibrium methods. These results also indicate that the CO formation proceeds via the initial formation of a five-coordinate  $\text{Co}^{\text{I}}\text{HMD}(\text{CO}_2)^+$  complex that quickly forms an equilibrium mixture with the six-coordinate complex,  $[\text{S-Co}^{\text{III}}\text{HMD}(\text{CO}_2^{2-})]^+$ . The production of CO in the photolysis solution likely proceeds by the subsequent reactions of  $[\text{S-Co}^{\text{III}}\text{HMD}(\text{CO}_2^{2-})]^+$  shown in Eqs 19 and 20.



The rate-determining step in the continuous photolysis system must be subsequent to the formation of the  $\text{S-CoHMD}(\text{CO}_2)^+$  and is likely to be the C–O bond breakage in the bound

carboxylic acid in Eq 20. Recent developments in transient FTIR may allow the study of the reactions  $S\text{-CoHMD}(\text{CO}_2)^+$  in the photocatalytic system.

Studies of catalytic systems with other cobalt macrocycles highlight some of the factors controlling the kinetics of the photoreduction of  $\text{CO}_2$ . Photogenerated  $\text{Co}^{\text{I}}\text{DMD}^+$  (lifetime 16  $\mu\text{s}$ ) is unstable while  $\text{Co}^{\text{I}}\text{OMD}^+$  is very stable (lifetime 6 h) in MeCN solution. The  $\text{CO}_2$  binding constants ( $K_{\text{CO}_2}$ ) are 6 and  $> 5 \times 10^4 \text{ M}^{-1}$  for  $\text{Co}^{\text{I}}\text{OMD}^+$  and  $\text{Co}^{\text{I}}\text{DMD}^+$ , respectively, at room temperature. While the DMD complex with no axial methyl groups prefers the 6-coordinate  $\text{CO}_2$  adduct, formation of the 6-coordinate  $S\text{-CoOMD}(\text{CO}_2)^+$  is unfavorable due to the steric hindrance of the four axial methyl groups. The  $\text{Co}^{\text{III}}$  redox potentials, the  $\text{CO}_2$  binding constants, and the lifetimes show a strong correlation:  $\text{Co}^{\text{I}}\text{OMD}^+$  (-1.28 V,  $6 \text{ M}^{-1}$ , 16  $\mu\text{s}$ ),  $\text{Co}^{\text{I}}\text{HMD}^+$  (-1.34 V,  $1.2 \times 10^4 \text{ M}^{-1}$ ,  $\sim 2 \text{ s}$ ) and  $\text{Co}^{\text{I}}\text{DMD}^+$  (-1.51 V,  $> 5 \times 10^4 \text{ M}^{-1}$ , 6 h).

#### 1.4.3 Systems with phenazine/ $\text{CoL}^{2+}$

Recently photoreduction of  $\text{CO}_2$  to  $\text{HCOO}^-$  (together with small amounts of CO and  $\text{H}_2$ ) has been achieved by UV-irradiation (313 nm) of a system involving phenazine as a photosensitizer,  $\text{Co}(\text{cyclam})^{3+}$  as an electron mediator and TEA as an electron donor<sup>[42]</sup>. The quantum yield for the formation of  $\text{HCOO}^-$  is 0.035. Electron transfer from the photogenerated radical anion ( $\text{Phena}^{\bullet-}$ ) to  $\text{Co}(\text{cyclam})^{3+}$  ( $k = 4.3 \times 10^9 \text{ M}^{-1} \text{ s}^{-1}$ ) results in the formation of  $\text{Co}(\text{cyclam})^{2+}$ . Since the reduction potential of  $\text{Co}(\text{cyclam})^{2+/+}$  is  $\sim -1.9 \text{ V}$  vs SCE in MeCN,  $\text{Phena}^{\bullet-}$  (-1.18 V vs SCE for a  $\text{Phena}/\text{Phena}^{\bullet-}$  couple), unlike  $\text{TP}^{\bullet-}$ , is hardly capable of reducing  $\text{Co}(\text{II})$  to  $\text{Co}(\text{I})$ . The authors suggest that:  $\text{PhenaH}^{\bullet}$ , produced by the protonation to  $\text{Phen}^{\bullet-}$ , may transfer a hydrogen atom to  $\text{Co}(\text{cyclam})^{2+}$  to form  $\text{Co}(\text{cyclam})(\text{H})^{2+}$  and insertion of  $\text{CO}_2$  into the hydride produces  $\text{HCOO}^-$  via the  $\text{Co}^{\text{III}}$ -formate complex. Although the results appear to support the proposed mechanism, the hydrogen-atom transfer step and the  $\text{CO}_2$  insertion step have not been investigated in detail.

## 2. *fac*- $\text{Re}(\alpha\text{-diimine})(\text{CO})_3\text{X}$ , $\text{Re}(\alpha\text{-diimine})(\text{CO})_2\text{XX}'$ or similar complexes

## 2.1 Overview of CO<sub>2</sub> reduction systems mediated rhenium complexes

Complexes of the general formula, *fac*-Re( $\alpha$ -diimine)(CO)<sub>3</sub>X and Re( $\alpha$ -diimine)(CO)<sub>2</sub>X(X') (where  $\alpha$ -diimine = bpy, phen, substituted bpy or phen, etc. and X, X' = halide, solvent, alkyl, benzyl, monodentate phosphine, CO, etc), have attracted interest since the mid-1970s<sup>[46-48]</sup>. Many of these complexes show emission from their lowest long-lived MLCT state at room temperature in solution. Their catalytic properties for CO<sub>2</sub> reduction have also been investigated. Electrolysis of a solution containing *fac*-Re(bpy)(CO)<sub>3</sub>Cl and 0.1 M Bu<sub>4</sub>NPF<sub>6</sub> in freshly distilled CO<sub>2</sub>-saturated MeCN at -1.5 V (vs SCE) produces both CO and CO<sub>3</sub><sup>2-</sup> with current efficiencies of 98% and 110 %, respectively<sup>[49]</sup>. Further, *fac*-Re(bpy)(CO)<sub>3</sub>X (X = Cl, Br) has been used successfully as a photocatalyst for CO<sub>2</sub> reduction to CO with TEOA in DMF<sup>[50-53]</sup>. When X = Cl, a quantum yield of 0.14 has been measured in the presence of excess Cl<sup>-</sup>. A formate-rhenium complex, *fac*-Re(bpy)(CO)<sub>3</sub>(O<sub>2</sub>CH), has been isolated in the absence of excess Cl<sup>-</sup>.

Among rhenium catalysts for the photochemical reduction of CO<sub>2</sub>, *fac*-Re(bpy)(CO)<sub>3</sub>{P(OEt)<sub>3</sub>}<sup>+</sup> is the best catalyst and irradiation of DMF solutions containing CO<sub>2</sub> and TEOA yields CO with a quantum yield of 0.38<sup>[54]</sup>. However, the formate complex *fac*-Re(bpy)(CO)<sub>3</sub>(O<sub>2</sub>CH) is also produced upon irradiation of Re(bpy)(CO)<sub>3</sub>(PR<sub>3</sub>)<sup>+</sup> (R = O-i-Pr, OEt, and Ph) in yields of 24, 73, and 55%, respectively, based on *fac*-Re(bpy)(CO)<sub>3</sub>(PR<sub>3</sub>)<sup>+</sup>. It is generally believed that the formate complex is produced by CO<sub>2</sub> insertion into a Re-H bond and leads to the production of free formate. However, neither electrochemical nor photochemical CO<sub>2</sub> reduction using *fac*-Re(bpy)(CO)<sub>3</sub>X produces any significant amount of formate. Despite the great interest in CO<sub>2</sub> utilization, the mechanism of CO formation with *fac*-Re(bpy)(CO)<sub>3</sub>X remains unclear. Below we discuss the possible involvement of intermediates such as Re-COO, Re-COOH, Re-CHO, Re-H, Re-CO, Re-O<sub>2</sub>COH, Re-CH<sub>2</sub>OH, etc.

## 2.2 Properties of Re( $\alpha$ -diimine)(CO)<sub>3</sub>X and Re( $\alpha$ -diimine)(CO)<sub>2</sub>XX'

### 2.2.1 Redox properties

The complexes can be both oxidized and reduced; reduction potentials for many of the complexes are shown in Table 6. Cyclic voltammograms of  $\text{Re}(\alpha\text{-diimine})(\text{CO})_3\text{X}$  show that in most cases the first oxidation is chemically irreversible at scan rates of 0.1 - 0.2 V/s; however, at much faster sweep rates ( $> 100$  V/s) a reversible wave is observed at 1.32 V (vs SCE) in MeCN for  $\text{Re}(\text{bpy})(\text{CO})_3\text{Cl}$ [55]. The first oxidation is metal based and is followed by the rapid loss of carbon monoxide due to the weakening of the Re  $\pi$ -backbonding to CO. Oxidation of *fac*- $\text{Re}(\text{bpy})(\text{CO})_3\text{H}$  occurs more easily than that of *fac*- $\text{Re}(\text{bpy})(\text{CO})_3\text{Cl}$  indicating the increased electron density on the Re center.

The electrochemical behavior of  $\text{Re}(\alpha\text{-diimine})(\text{CO})_3\text{X}$  in the negative potential region is usually shows three well-defined reduction waves. The first reduction wave is reversible and is assigned as a ligand-based reduction. The second wave is usually irreversible and assigned as a metal-based reduction followed by the rapid loss of X.

Spectroelectrochemical experiments using FTIR indicate that the reduced  $\text{Re}(\text{bpy})(\text{CO})_3\text{Cl}^-$  shows a significant shift of the CO vibrational frequencies to lower energy. The electron, while primarily residing in the bpy ligand  $\pi^*$  orbital, increases the amount of charge on the Re center by reducing Re-bpy  $\pi$ -backbonding. This increases Re-CO  $\pi$ -backbonding and raises the electron density in the  $\pi^*$  orbital of the CO, and thus decreases the CO bond strength and vibrational frequencies. The IR absorption of the CO,  $\nu_{\text{CO}}$ , shifts by about  $\approx 30 \text{ cm}^{-1}$  to lower energy.

The stability of the reduced complex depends on the ability of the X ligand to accommodate the increased electron density of the Re center. In the case of ligands that can not easily accept electron density into a low-energy orbital the increased electron density on the Re weakens the Re-X bond and can lead to loss of the X ligand. Complexes such as  $\text{Re}(\text{dmb})(\text{CO})_3\text{Cl}$  tend to form the five-coordinate radical  $[\text{Re}(\text{dmb})(\text{CO})_3]^\bullet$  species upon reduction even in MeCN[56]. This effect is stronger in the doubly reduced species that has an electron added directly to the Re center.

Table 6. Redox properties of  $[\text{Re}(\text{bpy})(\text{CO})_3\text{X}]^{\text{n}+}$  and  $[\text{Re}(\text{bpy})(\text{CO})_2\text{XX}']^{\text{n}+}$  vs SCE at room temperature

Complex	Solvent	$E_{1/2}$	Ref
		V	
$[\text{Re}(\text{bpy})(\text{CO})_3\text{Br}]$	THF	-1.91 <sup>a,b</sup> , -2.33 <sup>a,b</sup>	[57]
$[\text{Re}(\text{bpy})(\text{CO})_3\text{Cl}]$	THF	-1.91 <sup>a,b</sup> , -2.38 <sup>a,b</sup>	[57, 58]
$[\text{Re}(\text{bpy})(\text{CO})_3\text{Cl}]$	THF/MeCN	-1.76 <sup>b</sup> , -2.21 <sup>a,b</sup>	[56]
$[\text{Re}(\text{bpy})(\text{CO})_3\text{Cl}]$	THF	-1.91 <sup>a,b</sup>	[57]
$[\text{Re}(\text{bpy})(\text{CO})_3\text{Cl}]$	MeCN	1.32 <sup>c</sup> , -1.35 <sup>c</sup>	[49, 59]
$[\text{Re}(\text{bpy})(\text{CO})_3\text{Cl}]$	MeCN or DMF	1.36, -1.32	[60]
$[\text{Re}(\text{bpy})(\text{CO})_3\text{I}]$	THF	-1.91 <sup>a,b</sup> , -2.27 <sup>a,b</sup>	[57]
$[\text{Re}(\text{bpy})(\text{CO})_3(\text{H})]$	MeCN	0.90,	[61]
$[\text{Re}(\text{bpy})(\text{CO})_3(\text{H})]$	$\text{CH}_2\text{Cl}_2$	-1.46	[61]
$[\text{Re}(\text{bpy})(\text{CO})_3(\text{O}_2\text{CH})]$	MeCN	1.37, -1.29, -1.71	[61]
$[\text{Re}(\text{bpy})(\text{CO})_3(\text{O}_2\text{CH})]$	MeCN	-1.81 <sup>b</sup> , -2.33 <sup>a,b</sup>	[56]
$[\text{Re}(\text{bpy})(\text{CO})_3(\text{Otf})]$	THF	-1.54 <sup>a,b</sup>	[57]
$[\text{Re}(\text{bpy})(\text{CO})_3(\text{P}(\text{OEt})_3)]^+$	MeCN	1.6 <sup>d,e</sup> , -1.59 <sup>d</sup> , -2.1 <sup>a,d</sup>	[62]
$[\text{Re}(\text{bpy})(\text{CO})_3(\text{P}(\text{OEt})_3)]^+$	MeCN	-1.63 <sup>b</sup> , -2.40 <sup>a,b</sup>	[56]
$[\text{Re}(\text{bpy})(\text{CO})_3(\text{PPh}_3)]^+$	MeCN	1.6 <sup>d,e</sup> , -1.55 <sup>d</sup> , -1.98 <sup>a,d</sup>	[62]
$[\text{Re}(\text{bpy})(\text{CO})_3(\text{PPh}_3)]^+$	THF	-1.62 <sup>a,b</sup> , -2.10 <sup>a,b</sup>	[57]
$[\text{Re}(\text{bpy})(\text{CO})_3(\text{PPh}_3)]^+$	THF/MeCN	-1.58 <sup>b</sup> , -2.10 <sup>a,b</sup>	[56]
$[\text{Re}(\text{bpy})(\text{CO})_3(\text{MeCN})]^+$	THF/MeCN	-1.58 <sup>b</sup> , -1.80 <sup>a,b</sup>	[56]
$[\text{Re}(\text{bpy})(\text{CO})_3(\text{MeCN})]^+$	MeCN	-1.2	[63]
$[\text{Re}(\text{bpy})(\text{CO})_3(\text{PrCN})]^+$	PrCN	-1.62 <sup>a,b</sup> , -1.97 <sup>a,b</sup>	[58]

$[\text{Re}(\text{bpy})(\text{CO})_3(\text{THF})]^+$	THF		-1.73 <sup>a,b</sup> ,	-2.23 <sup>a,b</sup>	[57]
$[\text{Re}(\text{bpy})(\text{CO})_2(\text{P}(\text{OEt})_3)_2]^+$	MeCN		-1.69 <sup>d</sup> ,	-2.45 <sup>a,d</sup>	[64]
$[\text{Re}(\text{bpy})(\text{CO})_2(\text{P}(\text{OEt})_3)_2]^+$	MeCN		-1.79 <sup>b</sup> ,	-2.82 <sup>a,b</sup>	[56]
$[\text{Re}(\text{bpy})(\text{CO})_3]_2$	THF	-0.29 <sup>b,c</sup> ,	-0.6 <sup>b,c</sup> ,	-2.08 <sup>a,b</sup>	[57]
$[\text{Re}(\text{dmb})(\text{CO})_3\text{Cl}]$	MeCN	1.39 <sup>c</sup> ,	-1.43 <sup>c</sup> ,	-1.96 <sup>a,c</sup>	[55]
$[\text{Re}(\text{dmb})(\text{CO})_3\text{Cl}]$	MeCN or DMF		-1.32		[60]
$[\text{Re}(\text{dmb})(\text{CO})_3\text{Cl}]$	MeCN	1.3,	~-1.5,	~-1.8	[65]
$[\text{Re}(\text{phen})(\text{CO})_3\text{Cl}]$	MeCN or DMF	1.36,	-1.27		[60]
$[\text{Re}(\text{phen})(\text{CO})_3\text{Cl}]$	MeCN	1.33,	-1.34		[66]
$[\text{Re}(\text{phen})(\text{CO})_3(\text{P}(\text{OEt})_3)]^+$	MeCN		-1.55 <sup>d</sup>		[67]

<sup>a</sup> E<sub>pc</sub>. <sup>b</sup> vs Fc/Fc<sup>+</sup>. <sup>c</sup> vs SSCE. <sup>d</sup> vs Ag/AgNO<sub>3</sub>. <sup>e</sup> E<sub>pa</sub>.

Table 7. UV/vis Spectra and Lifetimes for *fac*-Re(CO)<sub>3</sub>( $\alpha$ -diimine)L Complexes

Complex	Solvent	$\lambda_{\max}$ nm	$\tau$ ns	$\lambda(\text{em})$ nm	Ref.
Re(4,4'-bpy) <sub>2</sub> (CO) <sub>3</sub> Cl	benzene		900/3300		[68]
Re(4,4'-bpy) <sub>2</sub> (CO) <sub>3</sub> Cl	CH <sub>2</sub> Cl <sub>2</sub>		1010		[69]
Re(4,4'-bpy) <sub>2</sub> (CO) <sub>3</sub> Cl	benzene		2100		[69]
Re(bpy)(CO) <sub>3</sub> Cl	CH <sub>2</sub> Cl <sub>2</sub>	385	51	622	[59]
Re(bpy)(CO) <sub>3</sub> Cl	MeCN	370	25	622	[60]
Re(bpy)(CO) <sub>3</sub> Cl	MeCN	370, 318, 295	25/33		[70]
Re(bpy)(CO) <sub>3</sub> Cl	DMF	373	26	620	[60]
Re(bpy)(CO) <sub>3</sub> Cl	EtOH	372	36	610	[60]
Re(bpy)(CO) <sub>3</sub> Cl	CH <sub>2</sub> Cl <sub>2</sub>	384	50	615	[60]
Re(bpy)(CO) <sub>3</sub> Cl	THF	388	65	622	[60]
Re(bpy)(CO) <sub>3</sub> Cl	dioxane	390	62	626	[60]
Re(bpy)(CO) <sub>3</sub> Cl	benzene	400	70	615	[60]
Re(bpy)(CO) <sub>3</sub> Cl <sup>a</sup>	MeTHF	375	2700	532	[71]
Re(bpy)(CO) <sub>3</sub> (MeCN) <sup>+</sup>	CH <sub>2</sub> Cl <sub>2</sub>	343	1201	536	[59]
Re(bpy)(CO) <sub>3</sub> (Otf)	THF	355			[57]

Re(bpy)(CO) <sub>3</sub> (O <sub>2</sub> CH)	CH <sub>2</sub> Cl <sub>2</sub>	382			[61]
Re(bpy)(CO) <sub>3</sub> (O <sub>2</sub> COH)	DMSO	362			[61]
Re(bpy)(CO) <sub>3</sub> (H)	CH <sub>2</sub> Cl <sub>2</sub>	415			[61]
Re(bpy)(CO) <sub>3</sub> (THF) <sup>+</sup>	THF	385			[57]
Re(bpy)(CO) <sub>3</sub> Br <sup>a</sup>	MeTHF	378	3700	530	[71]
Re(bpy)(CO) <sub>3</sub> Br	DMF	375	55	610	[52]
Re(bpy)(CO) <sub>3</sub> I	THF	320 sh, 403			[71]
Re(bpy)(CO) <sub>3</sub> I <sup>a</sup>	MeTHF	388	7500	525	[71]
Re(bpy)(CO) <sub>3</sub> CH <sub>3</sub>	MeCN	410, 270			[70]
Re(bpy)(CO) <sub>3</sub> P(CH <sub>3</sub> ) <sub>3</sub> <sup>†</sup>	CH <sub>2</sub> Cl <sub>2</sub>	358	1169	544	[59]
Re(bpy)(CO) <sub>3</sub> {P(OEt <sub>3</sub> ) <sub>3</sub> } <sup>+</sup>	MeCN	317, 351 sh	920	521	[54]
Re(bpy)(CO) <sub>3</sub> PPh <sub>3</sub> <sup>+</sup>	THF	365, 330			[57]
Re(bpy)(CO) <sub>3</sub> PPh <sub>3</sub> <sup>+</sup>			416	517	[72]
Re(dmb)(CO) <sub>3</sub> Cl	MeCN	360	27	592	[60]
Re(dmb)(CO) <sub>3</sub> CH <sub>3</sub>	CH <sub>2</sub> Cl <sub>2</sub>		35		[73]
Re(dmb)(CO) <sub>3</sub> CH <sub>3</sub>	toluene		40		[73]
Re(dmb)(CO) <sub>3</sub> CH <sub>3</sub>	THF		30		[73]
Re(dmb)(CO) <sub>3</sub> CH <sub>3</sub> <sup>a</sup>	MeTHF	398	5000	644	[73]
Re(phen)(CO) <sub>3</sub> (MeCN) <sup>+</sup>	MeCN	360	2400	532	[63]

Re(phen)(CO) <sub>3</sub> Cl	MeCN	364	178	612	[60]
Re(phen)(CO) <sub>3</sub> Cl	DMF	366	155	614	[60]
Re(phen)(CO) <sub>3</sub> Cl	EtOH	369	216	600	[60]
Re(phen)(CO) <sub>3</sub> Cl	CH <sub>2</sub> Cl <sub>2</sub>	374	288	604	[60]
Re(phen)(CO) <sub>3</sub> Cl	THF	382	335	622	[60]
Re(phen)(CO) <sub>3</sub> Cl	dioxane	384	340	620	[60]
Re(phen)(CO) <sub>3</sub> Cl	benzene	388	320	610	[60]

---

<sup>a</sup> 80 K.

Table 8. Re(CO)<sub>3</sub>bpyL Complexes CO Stretches

<i>Complexes</i>	Solvent	CO $\nu_{\max}$ , cm <sup>-1</sup>	CO or Other $\nu_{\max}$ , cm <sup>-1</sup>	Other $\nu_{\max}$ , cm <sup>-1</sup>	Ref.
Ground-state Complexes					
[Re(4,4-bpy) <sub>2</sub> (CO) <sub>3</sub> (MeCN)] <sup>+</sup>	KBr	2043, 1930 br,			[74]
[Re(4,4-bpy) <sub>2</sub> (CO) <sub>3</sub> (MeCN)] <sup>+</sup>	MeCN	2046, 1942 br,			[74]
[Re(4,4-bpy) <sub>2</sub> (CO) <sub>3</sub> Cl]	CH <sub>2</sub> Cl <sub>2</sub>	2027, 1926, 1891			[69, 75, 76]
[Re(4,4-bpy) <sub>2</sub> (CO) <sub>3</sub> Cl]	MeCN	2026, 1922, 1895			[75, 76]
[Re(4,4-bpy) <sub>2</sub> (CO) <sub>3</sub> Cl]	MeCN	2028, 1923, 1892			[74]
[Re(4,4-bpy) <sub>2</sub> (CO) <sub>3</sub> Cl]	KBr	2017, 1892 br,			[74]
[Re(4,4-bpy) <sub>2</sub> (CO) <sub>3</sub> Cl] <sup>-</sup>	MeCN	2012, 1903, 1882			[75, 76]
[Re(4,4-bpy) <sub>2</sub> (CO) <sub>3</sub> Cl] <sup>2-</sup>	MeCN	2002, 1890, 1868			[75, 76]
[Re(bpy)(CO) <sub>3</sub> (MeCN)] <sup>+</sup>	KBr	2040, 1954, 1929	1920		[74]
[Re(bpy)(CO) <sub>3</sub> (MeCN)] <sup>+</sup>	MeCN	2041, 1936 br,			[74]
[Re(bpy)(CO) <sub>3</sub> ] <sup>-</sup>	PrCN (183 K)	1944, 1843 br,			[58]
[Re(bpy)(CO) <sub>3</sub> ] <sup>-</sup>	THF	1947, 1843 br,			[57]
[Re(bpy)(CO) <sub>3</sub> ] <sup>-</sup>	MeCN	1948, 1846,			[56, 76]
[Re(bpy)(CO) <sub>3</sub> (Br)]	THF	2019, 1919, 1895			[57]
[Re(bpy)(CO) <sub>3</sub> (Br)] <sup>-</sup>	THF	1997, 1888, 1867			[57]
[Re(bpy)(CO) <sub>3</sub> Cl]	KBr	2012, 1903, 1880			[74]
[Re(bpy)(CO) <sub>3</sub> Cl]	PrCN (213 K)	2021 s, 1916 m, 1897 m			[58]
[Re(bpy)(CO) <sub>3</sub> Cl]	CH <sub>2</sub> Cl <sub>2</sub>	2024, 1921, 1899			[75, 76]
[Re(bpy)(CO) <sub>3</sub> Cl]	CH <sub>2</sub> Cl <sub>2</sub>	2020, 1920, 1900			[77]

[Re(bpy)(CO) <sub>3</sub> Cl]	DMF	2019, 1914, 1893			[51, 57, 77]
[Re(bpy)(CO) <sub>3</sub> Cl]	THF	2019, 1917, 1895			[57]
[Re(bpy)(CO) <sub>3</sub> Cl]	MeCN	2023, 1916, 1902			[74]
[Re(bpy)(CO) <sub>3</sub> Cl]	MeCN	2023, 1917, 1899 m			[57, 76]
[Re(bpy)(CO) <sub>3</sub> Cl]	MeCN	2021 s, 1914 m, 1897 m			[56]
[Re(bpy)(CO) <sub>3</sub> Cl] <sup>-</sup>	PrCN (213 K)	1996 s, 1881 m, 1865 m			[58]
[Re(bpy)(CO) <sub>3</sub> Cl] <sup>-</sup>	MeCN	1996, 1881, 1867			[75, 76]
[Re(bpy)(CO) <sub>3</sub> Cl] <sup>-</sup>	MeCN	1998 s, 1880 m, 1866 m			[74]
[Re(bpy)(CO) <sub>3</sub> Cl] <sup>-</sup>	DMF	1994, 1880, 1862			[57, 77]
[Re(bpy)(CO) <sub>3</sub> Cl] <sup>-</sup>	THF	1996, 1883, 1868			[57]
[Re(bpy)(CO) <sub>3</sub> Cl] <sup>-</sup>	MeCN	1998, 1885, 1868			[56]
[Re(bpy)(CO) <sub>3</sub> I]	THF	2020, 1921, 1900			[57]
[Re(bpy)(CO) <sub>3</sub> I] <sup>-</sup>	THF	1995, 1889, 1866			[57]
[Re(bpy)(CO) <sub>3</sub> (O <sub>2</sub> CH)]	KBr	2020, 1920, 1880	1630	1280	[51]
[Re(bpy)(CO) <sub>3</sub> (O <sub>2</sub> CH)]	KBr	2018, 1918, 1893	1633	1281	[74]
[Re(bpy)(CO) <sub>3</sub> (O <sub>2</sub> CH)]	THF	2019, 1916, 1894	1630	1280	[56]
[Re(bpy)(CO) <sub>3</sub> (O <sub>2</sub> CH)] <sup>-</sup>	THF	1997, 1879 br,	1628	1280	[56]
[Re(bpy)(CO) <sub>3</sub> (CH <sub>2</sub> OH)]	KCl	2017, 1997, 1885	1696		[78]
[Re(bpy)(CO) <sub>3</sub> (Otf)]	THF	2034, 1930, 1914			[57]
[Re(bpy)(CO) <sub>3</sub> (PPh <sub>3</sub> ) <sup>+</sup>	THF	2037, 1950, 1922			[57]
[Re(bpy)(CO) <sub>3</sub> (PPh <sub>3</sub> ) <sup>+</sup>	THF	2015, 1919, 1892			[57]
[Re(bpy)(CO) <sub>3</sub> (PrCN)] <sup>+</sup>	PrCN	2039 s, 1936 s, br,			[58]
[Re(bpy)(CO) <sub>3</sub> (PrCN)] <sup>+</sup>	PrCN	201, 1905, 1885			[58]
[Re(bpy)(CO) <sub>3</sub> (PrCN)] <sup>-</sup>	PrCN (183 K)	1980, 1861, 1851			[58]
[Re(bpy)(CO) <sub>3</sub> (THF)] <sup>+</sup>	THF	2019, 1917, 1894			[57]
[Re(bpy)(CO) <sub>2</sub> {P(OEt) <sub>3</sub> } <sub>2</sub> ]Br	CH <sub>2</sub> Cl <sub>2</sub>	1956, 1882,			[64]

$[\text{Re}(\text{dmb})(\text{CO})_3(\text{CH}_3)]$	EtCN/PrCN (195 K)	1987, 1874, 1867			[73]
$[\text{Re}(\text{dmb})(\text{CO})_3(\text{MeCN})]^+$	MeCN	2039, 1934 br,			[74]
$[\text{Re}(\text{dmb})(\text{CO})_3(\text{MeCN})]^+$	MeCN	2039, 1948, 1935			[65]
$[\text{Re}(\text{dmb})(\text{CO})_3]$	MeCN	1979, 1876, 1843			[65]
$[\text{Re}(\text{dmb})(\text{CO})_3]_2$	KBr	2020, 1940, 1860			[51]
$[\text{Re}(\text{dmb})(\text{CO})_3]_2$	MeCN	(1975), 1943,			[65]
$[\text{Re}(\text{dmb})(\text{CO})_3]^-$	MeCN	1943, 1828,			[65]
$[\text{Re}(\text{dmb})(\text{CO})_3]_2^-$	MeCN	1960, 1930, 1865	1830		[65]
$[\text{Re}(\text{dmb})(\text{CO})_3\text{Cl}]$	MeCN	2023, 1906, 1893			[65]
$[\text{Re}(\text{dmb})(\text{CO})_3\text{Cl}]$	MeCN	2021, 1914, 1898			[74]
$[\text{Re}(\text{dmb})(\text{CO})_3\text{Cl}]^-$	MeCN	1993, 1875,			[65]
$[\text{Re}(\text{dmb})(\text{CO})_3(\text{CO}_2\text{H})]$	KCl	2012, 1916, 1892	1572	1194	[79]
$[\text{Re}(\text{dmb})(\text{CO})_3(\text{CO}_2\text{H})]$ or $[\text{Re}(\text{dmb})(\text{CO})_3(\text{CO}_2)]$	MeCN	2010, 1902, 1878			[65]
$[\text{Re}(\text{dmb})(\text{CO})_3(\text{CO}_2\text{H})]^-$	MeCN	1997, 1860,			[65]
$[\text{Re}(\text{dmb})(\text{CO})_3(\text{CO}_2\text{H})]^-$	THF	2014, 1916, 1894			[57]
$[\text{Re}(\text{dmb})(\text{CO})_3(\text{CO}_2\text{H})]^-$	MeCN	1986, 1868, 1852			[57]
$[\text{Re}(\text{dmb})(\text{CO})_3]_2(\text{CO}_2)$	KCl	1992, 1888, 1866	1485	1155	[79]
$[\text{Re}(\text{dmb})(\text{CO})_3\text{H}]$	KCl	1992, 1887, 1865	2019	2036	[79]
			(ReH)	(ReH)	
$[\text{Re}(\text{dmb})(\text{CO})_3\text{H}]$		1993, 1905, 1888	2018		[61]
			(ReH)		

Excited-state Complexes

*[Re(CO) <sub>3</sub> (4,4-bpy) <sub>2</sub> (MeCN)] <sup>+</sup>	MeCN	2068(22), 2031(89), 1992(50)	[74]
*[Re(CO) <sub>3</sub> (4,4-bpy) <sub>2</sub> Cl]	CH <sub>2</sub> Cl <sub>2</sub>	2055(28), 1992(66), 1957(66)	[69, 75, 76]
*[Re(CO) <sub>3</sub> (4,4-bpy) <sub>2</sub> Cl]	MeCN	2065(37), 1993(70), 1961(69)	[74]
*[Re(bpy)(CO) <sub>3</sub> (MeCN)] <sup>+</sup>	CH <sub>2</sub> Cl <sub>2</sub>	2071(36), 2018(81), 1984(49)	[80]
*[Re(bpy)(CO) <sub>3</sub> (MeCN)] <sup>+</sup>	MeCN	2070(29), 2017(80), 1982(47)	[74]
*[Re(bpy)(CO) <sub>3</sub> Cl]	CH <sub>2</sub> Cl <sub>2</sub>	2065(45), 1991(71), 1951(51)	[81]
*[Re(bpy)(CO) <sub>3</sub> Cl]	CH <sub>2</sub> Cl <sub>2</sub>	2064(40), 1987(66), 1957(58)	[76]
*[Re(bpy)(CO) <sub>3</sub> Cl]	MeCN	2067(44), 1990(76), 1874(73)	[74]
*[Re(bpy)(CO) <sub>2</sub> {P(OEt) <sub>3</sub> } <sub>2</sub> ]Br	CH <sub>2</sub> Cl <sub>2</sub>	2012(56), 1927(45),	[64]
*[Re(dmb)(CO) <sub>3</sub> (CH <sub>3</sub> )]	EtCN/PrCN (195 K)	2029(42), 1950(76), 1925(58)	[73]
*[Re(dmb)(CO) <sub>3</sub> (MeCN)] <sup>+</sup>	MeCN	2062(23), 2013(79), 1973(45)	[74]
*[Re(dmb)(CO) <sub>3</sub> Cl]	MeCN	2062(41), 1989(75), 1953(55)	[74]



### 2.2.2. Excited-state photochemistry and photophysics

The photophysical properties of low-spin  $d^6$  complexes, *fac*-Re( $\alpha$ -diimine)(CO)<sub>3</sub>X, are summarized in Table 7. These complexes are often emissive in solution and generally have an intense MLCT absorptions ( $Re^I d\pi \rightarrow \pi^*$  ( $\alpha$ -diimine)) between 340 and 500 nm depending on the  $\alpha$ -diimine, X ligands, and the solvent<sup>[48, 60]</sup>. Changes in solvent polarity lead to pronounced shifts of the absorption maxima (e.g. 370 nm in MeCN to 400 nm in benzene for Re(bpy)(CO)<sub>3</sub>Cl) as shown in Table 7<sup>[47]</sup>). Modification of the  $\alpha$ -diimine ligand also affects the MLCT absorption with the  $\lambda_{max}$  shifting to shorter wavelength in the order *dmb* > *phen* > *bpy*<sup>[47, 48]</sup>. The replacement of Cl<sup>-</sup> by I<sup>-</sup> changes the excited-state character from MLCT to XLCT (X = halide)<sup>[71]</sup>. The MLCT absorption of Re(bpy)(CO)<sub>3</sub>X (X = H or CH<sub>3</sub>) is red shifted compared to that of Re(bpy)(CO)<sub>3</sub>Cl. An excellent review of the photophysics of these complexes by Stufken and Vlcek has recently been published<sup>[48]</sup>.

For *fac*-Re( $\alpha$ -diimine)(CO)<sub>3</sub>Cl the initial absorption at  $\approx 400$  nm populates a short-lived <sup>1</sup>MLCT state. This state rapidly decays to the long lived <sup>3</sup>MLCT states. These states are actually three closely-spaced levels split by spin-orbit coupling. Since the splitting is small the states behave kinetically as a single level at temperatures above 77 K<sup>[48]</sup>. The <sup>3</sup>MLCT excited state can be viewed as a charge-separated species  $*[Re^{II}(\alpha\text{-diimine}^-)(CO)_3Cl]$ . Transient UV-vis spectra show that the excited-state absorption corresponds to the  $\alpha$ -diimine<sup>-</sup> anion chromophore<sup>[60]</sup>. Transient IR spectroscopy of the excited state shows a significant shift (20 to 80  $cm^{-1}$ ) of the CO vibrational frequencies to higher energy. The shift is similar but smaller to that observed on oxidation of the Re( $\alpha$ -diimine)(CO)<sub>3</sub>Cl complex<sup>[65]</sup>. The charge transfer in the excited state decreases the amount of charge on the Re center. This reduces the  $\pi$ -backbonding between the Re center and the CO ligands thereby increasing the CO bond strength and vibrational frequencies. Similar effects have also been observed in the time-resolved resonance Raman spectroscopy<sup>[48]</sup>.

The complexes often undergo radiative decay from their lowest excited state both in fluid solutions at room temperature and in glassy media at 77 K[46, 48, 59, 66]. Emission lifetimes are typically 20 ns to 1  $\mu$ s at room temperature and are summarized in Table 7. The excited state can decay by two nonradiative pathways: by internal conversion to the ground state and by a thermally activated process through a higher energy excited state that rapidly decays to the ground state. The exact parameters for the two pathways depend on X, L, solvent, and temperature.

The  $^3$ MLCT excited state is both a strong oxidant and a strong reductant and it can be quenched by either electron acceptors (oxidative) or donors (reductive quenching)[60, 66]. Table 9 indicates rate constants for oxidative and reductive quenching of MLCT excited state of a number of *fac*-Re( $\alpha$ -diimine)(CO)<sub>3</sub>X complexes.

Table 9. Oxidative and Reductive Quenching of MLCT excited state of  $\text{Re}(\text{CO})_3\text{LX}$  by Q to Produce the Oxidized Re complex and  $\text{Q}^-$  in MeCN at room temperature.

L	X	Q	$E^\circ$ vs SCE V	$k_q \times 10^9$ $\text{M}^{-1} \text{s}^{-1}$	Ref
Oxidative Quenching					
phen	Cl	tetracyanoethylene	+0.24	7.4	[66]
phen	Cl	1,1'-propylene-1,10-phenanthroline HFP	-0.27	3.3	[66]
phen	Cl	1,1'-ethylene-2,2'-bipyridinium HFP	-0.36	3.6	[66]
phen	Cl	N,N'-dibenzyl-4,4'-bipyridinium HFP	-0.36	2.7	[66]
phen	Cl	N,N'-dimethyl-4,4'-bipyridinium HFP	-0.45	3.1	[66]
phen	Cl	N-methyl-4-cyanopyridinium HFP	-0.79	2.3	[66]
phen	Cl	p-nitrobenzaldehyde	-0.86	2.6	[66]
phen	Cl	N-methyl-4-carbomethoxypyridinium HFP	-0.93	1.7	[66]
phen	Cl	4,4'-dinitrobiphenyl	-1.0	1.9	[66]
phen	Cl	m-nitrobenzaldehyde	-1.02	0.64	[66]
phen	Cl	4-chloronitrobenzene	-1.06	0.24	[66]

phen	Cl	4-methylnitrobenzene	-1.20	<0.02	[66]
Ph <sub>2</sub> phen	Cl	N,N'-dibenzyl-4,4'- bipyridinium HFP	-0.36	3.3	[66]
Ph <sub>2</sub> phen	Cl	N,N'-dimethyl-4,4'- bipyridinium HFP	-0.45	3.5	[66]

---

Reductive Quenching

phen	Cl	N,N,N',N'-tetramethyl-p- phenylenediamine	+0.24	5.7	[66]
phen	Cl	N,N'-diphenyl-p- phenylenediamine	+0.35	3.7	[66]
phen	Cl	N,N-dimethyl-p-toluidine	+0.65	2.1	[66]
phen	Cl	10-methylphenathiazine	+0.83	1.7	[66]
phen	Cl	N,N-dimethylaniline	+0.78	0.98	[66]
phen	Cl	diphenylamine	+0.83	0.40	[66]
phen	Cl	triphenylamine	+0.86	0.33	[66]
phen	Cl	aniline	+0.98	0.058	[66]
phen	Cl	p-bromoaniline	+0.97	0.054	[66]
phen	Cl	N,N-dimethylbenzylamine	+1.01	<0.002	[66]
phen	Cl	p-dimethoxybenzene	+1.34	<0.002	[66]
phen	Cl	N,N-dimethylaniline	+0.78	0.98	[60]
phen	Cl	diphenylamine	+0.83	0.4	[60]
phen	Cl	N,N',N'-triphenylamine	+0.98	0.33	[60]
pdphen	Cl	N,N,N',N'-tetramethyl-p- phenylenediamine	+0.24	8.7	[66]
Ph <sub>2</sub> phen	Cl	N,N-dimethyl-p-toluidine	+0.65	3.9	[66]

Ph <sub>2</sub> phen	Cl	aniline	+0.98	0.20	[66]
Ph <sub>2</sub> phen	Cl	p-dimethoxybenzene	+1.34	<0.002	[66]
bpy	Cl	TEOA	+0.80	0.08	[60]
bpy	{P(OEt) <sub>3</sub> } <sub>2</sub>	DABCO (1,4-diazabicyclo[2.2.2]octane)		0.28	[64]
bpy	P(OEt) <sub>3</sub>	TEOA	+0.80	1.1	[67]
bpy	P(OEt) <sub>3</sub>	TEOA	+0.80	0.8	[54]
bpy	Cr	TEOA	+0.80	0.06	[52]

---

The relationship between the absorption ( $E_{\text{abs}}$ ), emission ( $E_{\text{em}}$ ), reorganization ( $\lambda_r$ ), the singlet-triplet splitting ( $E_{\text{st}}$ ) energies<sup>[82]</sup> and the energy difference between the thermally relaxed excited and ground states ( $E_{0-0}$ ) is shown in Figure 8<sup>[83]</sup>.

$$E_{\text{abs}} = E_{\text{em}} + E_{\text{st}} + 2\lambda_r$$

The reorganization energy,  $\lambda_r$ , is generally broken into contributions from the solvent and/or low-frequency internal modes of the complex,  $\lambda_s$ , and from the internal high-frequency modes of the complex,  $\lambda_i$ , with the total reorganization energy given by  $\lambda_r = \lambda_s + \lambda_i$ . A spherical continuum model<sup>[84]</sup> can be used to estimate the solvent contribution to  $\lambda_s$ . Using this model<sup>[85]</sup>  $\lambda_s = 0.18$  eV for  $\text{Ru}(\text{bpy})_3^{2+/*}$  in  $\text{H}_2\text{O}$  and 0.33 and 0.22 eV for  $\text{Re}(\text{bpy})(\text{CO})_3\text{Cl}$  in  $\text{H}_2\text{O}$  and  $\text{CH}_2\text{Cl}_2$ , respectively. The larger value for the Re (vs the Ru) complex is due to its smaller size while the decrease in the value of  $\lambda_s$  on going from water to  $\text{CH}_2\text{Cl}_2$  reflects the decrease in the polarity of the solvent.

An alternative method of estimating the reorganization energies involves spectral fitting of the emission<sup>[86, 87]</sup>. For a number of rhenium complexes the  $\lambda_s$  and  $\lambda_r$  values are given in Table 10. In general, similar  $\lambda_s$  values are estimated by either method with  $\lambda_s$  typically being about half of the total reorganization energy. As expected, the inner-shell reorganization energy for the Re carbonyl complexes is significant as indicated by the shifts in the  $\nu_{\text{CO}}$  frequencies. The  $E_{0-0}$  and the  $E_{\text{st}}$  are estimated for a number of complexes in Table 10. One notes that  $E_{\text{st}}$  is approximately constant for the  $\text{Ru}(\text{bpy})(\text{CO})_3\text{Cl}$  and  $\text{Ru}(\text{phen})(\text{CO})_3\text{Cl}$  complexes if one excludes the two nonpolar solvents. The excited state energies,  $E_{0-0}$  are important since they can be used to estimate the redox potential of the excited state.

Table 10. Reorganization Energies, Excited-State Energies and Singlet-Triplet Splitting for  $\text{Re}(\alpha\text{-diimine})(\text{CO})_3\text{X}$  Complexes.<sup>a</sup>

L	X	Solvent	$E_{\text{abs}}$ eV	$E_{\text{em}}$ eV	$\lambda_{\text{s}}$ eV	$\lambda_{\text{r}}$ eV	$E_{0-0}$ eV	$E_{\text{st}}$ eV	Ref
bpy	Cl	$\text{CH}_2\text{Cl}_2$	3.22	1.99	0.22 <sup>a</sup>	0.42 <sup>b</sup>	2.41	0.39	[60]
bpy	Cl	MeCN	3.35	1.99	0.31 <sup>a</sup>	0.51 <sup>b</sup>	2.50	0.34	[60]
bpy	Cl	DMF	3.32	2.00	0.28 <sup>a</sup>	0.48 <sup>b</sup>	2.48	0.36	[60]
bpy	Cl	METHF	3.10	1.93		0.44	2.37	0.29	[88]
bpy	Cl	EtOH	3.33	2.03	0.30 <sup>a</sup>	0.5 <sup>b</sup>	2.53	0.30	[60]
bpy	Cl	$\text{CH}_2\text{Cl}_2$	3.23	2.02	0.22 <sup>a</sup>	0.42 <sup>b</sup>	2.44	0.37	[60]
bpy	Cl	$\text{CH}_2\text{Cl}_2$	3.21	1.99	0.22 <sup>a</sup>	0.42	2.41	0.38	[59]
bpy	Cl	THF	3.20	1.99	0.21 <sup>a</sup>	0.41 <sup>b</sup>	2.40	0.38	[60]
bpy	Cl	dioxane	3.18	1.98	0.02 <sup>a</sup>	0.22 <sup>b</sup>	2.20	0.76	[60]
bpy	Cl	benzene	3.10	2.02	0.00 <sup>a</sup>	0.20 <sup>b</sup>	2.22	0.68	[60]
phen	Cl	MeCN	3.41	2.03	0.31 <sup>a</sup>	0.51 <sup>b</sup>	2.54	0.36	[60]
phen	Cl	DMF	3.39	2.02	0.28 <sup>a</sup>	0.48 <sup>b</sup>	2.50	0.41	[60]
phen	Cl	EtOH	3.36	2.07	0.30 <sup>a</sup>	0.50 <sup>b</sup>	2.57	0.29	[60]
phen	Cl	$\text{CH}_2\text{Cl}_2$	3.32	2.05	0.22 <sup>a</sup>	0.42 <sup>b</sup>	2.47	0.42	[60]
phen	Cl	$\text{CH}_2\text{Cl}_2$	3.03	2.15	0.22 <sup>a</sup>	0.42 <sup>b</sup>	2.57	0.02	[46]

phen	Cl	THF	3.25	1.99	0.21 <sup>a</sup>	0.41 <sup>b</sup>	2.40	0.43	[60]
phen	Cl	dioxane	3.23	2.00	0.02 <sup>a</sup>	0.22 <sup>b</sup>	2.22	0.79	[60]
phen	Cl	benzene	3.20	2.03	0.00 <sup>a</sup>	0.20 <sup>b</sup>	2.23	0.76	[60]
bpy	MeCN	CH <sub>2</sub> Cl <sub>2</sub>	3.61	2.31	0.22 <sup>a</sup>	0.42 <sup>b</sup>	2.73	0.46	[59]
bpy	Br	DMF	3.31	2.03	0.28 <sup>a</sup>	0.48 <sup>b</sup>	2.51	0.31	[52]
bpy	P(CH <sub>3</sub> ) <sub>3</sub>	CH <sub>2</sub> Cl <sub>2</sub>	3.46	2.28	0.22 <sup>a</sup>	0.42 <sup>b</sup>	2.70	0.34	[59]
bpy	P(OEt <sub>3</sub> )	MeCN	3.91	2.38	0.25 <sup>a</sup>	0.45 <sup>b</sup>	2.83	0.62	[54]
bpy	NH <sub>2</sub> py	CH <sub>2</sub> Cl <sub>2</sub>	3.31	2.08	0.22 <sup>a</sup>	0.42 <sup>b</sup>	2.50	0.39	[59]
bpy	Meimz	CH <sub>2</sub> Cl <sub>2</sub>	3.42	2.11	0.22 <sup>a</sup>	0.42 <sup>b</sup>	2.53	0.47	[59]
bpy	Etpy	CH <sub>2</sub> Cl <sub>2</sub>	3.43	2.19	0.22 <sup>a</sup>	0.42 <sup>b</sup>	2.61	0.41	[59]
bpy	py	CH <sub>2</sub> Cl <sub>2</sub>	3.45	2.22	0.22 <sup>a</sup>	0.42 <sup>b</sup>	2.64	0.39	[59]
bpy	P(CH <sub>2</sub> ) <sub>3</sub>	CH <sub>2</sub> Cl <sub>2</sub>	3.46	2.28	0.22 <sup>a</sup>	0.42 <sup>b</sup>	2.70	0.34	[59]
bpy	MeCN	CH <sub>2</sub> Cl <sub>2</sub>	3.61	2.31	0.22 <sup>a</sup>	0.42 <sup>b</sup>	2.73	0.46	[59]
bpy	3Mepy	MeCN	3.41	2.19	0.20	0.42	2.61	0.38	[89]
bpy	py	MeCN	3.39	2.22	0.20	0.44	2.66	0.29	[89]
bpy	3HOpy	MeCN	3.56	2.17	0.22	0.42	2.59	0.56	[89]
bpy	2Mepy	MeCN	3.41	2.21	0.20	0.42	2.63	0.35	[89]
bpy	2Mepy	CH <sub>2</sub> Cl <sub>2</sub>	3.25	2.03	0.22 <sup>a</sup>	0.42 <sup>b</sup>	2.45	0.37	[59]
bpy	4Etpy	EtOH/MeOH		2.11	0.21	0.51	2.45 <sup>b</sup>		[90]

dmb	Cl	MeCN	3.44	2.09	0.31 <sup>a</sup>	0.51 <sup>b</sup>	2.60	0.33	[60]
phen	MeCN	MeCN	3.44	2.33	0.31 <sup>a</sup>	0.51 <sup>b</sup>	2.84	0.09	[63]
dmb	py	MeCN	3.48	2.25	0.18	0.42	2.65	0.44	[89]
Ph <sub>2</sub> bpy	py	MeCN	3.48	2.18	0.15	0.37	2.55	0.56	[89]
phen	py	MeCN	3.37	2.28	0.22	0.44	2.72	0.21	[89]
phen	3Mepy	MeCN	3.23	2.25	0.20	0.42	2.67	0.14	[89]
Phphen	py	MeCN	3.76	2.28	0.16	0.38	2.66	0.72	[89]
Mephen	Cl	CH <sub>2</sub> Cl <sub>2</sub>	2.95	2.11	0.22 <sup>a</sup>	0.42 <sup>b</sup>	2.53	0.04	[46]
Ph <sub>2</sub> phen	Cl	CH <sub>2</sub> Cl <sub>2</sub>		2.14	0.22 <sup>a</sup>	0.42 <sup>b</sup>	2.51		[46]
Clphen	Cl	CH <sub>2</sub> Cl <sub>2</sub>	2.95	2.12	0.22 <sup>a</sup>	0.42 <sup>b</sup>	2.54		[46]
Brphen	Cl	CH <sub>2</sub> Cl <sub>2</sub>	2.98	2.12	0.22 <sup>a</sup>	0.42 <sup>b</sup>	2.54	0.01	[46]
dpp	Cl	CH <sub>2</sub> Cl <sub>2</sub>		1.72	0.39	0.47	2.19		[91]
dpp	Meimz	CH <sub>2</sub> Cl <sub>2</sub>		1.86	0.39	0.48	2.34		[91]
dpp	py	CH <sub>2</sub> Cl <sub>2</sub>		1.98	0.34	0.44	2.42		[91]
dpp	4Mepy	CH <sub>2</sub> Cl <sub>2</sub>		1.97	0.36	0.45	2.42		[91]
dpp	4Phpy	CH <sub>2</sub> Cl <sub>2</sub>		1.96	0.36	0.46	2.42		[91]
dpp	P(CH <sub>3</sub> ) <sub>3</sub>	CH <sub>2</sub> Cl <sub>2</sub>		2.05	0.34	0.37	2.42		[91]
dpp	MeCN	CH <sub>2</sub> Cl <sub>2</sub>		1.98	0.36	0.45	2.43		[91]

dpq	Meimz	CH <sub>2</sub> Cl <sub>2</sub>	1.60	0.45	0.47	2.07		[91]	
dpq	py	CH <sub>2</sub> Cl <sub>2</sub>	1.69	0.48	0.50	2.19		[91]	
dpq	4Mepy	CH <sub>2</sub> Cl <sub>2</sub>	1.68	0.48	0.49	2.17		[91]	
dpq	4Phpy	CH <sub>2</sub> Cl <sub>2</sub>	1.68	0.48	0.50	2.18		[91]	
dpq	P(CH <sub>3</sub> ) <sub>3</sub>	CH <sub>2</sub> Cl <sub>2</sub>	1.69	0.52	0.54	2.23		[91]	
dpq	MeCN	CH <sub>2</sub> Cl <sub>2</sub>	1.74	0.59	0.61	2.35		[91]	
(NEt <sub>2</sub> ) <sub>2</sub> bpy	Cl	MeTHF	3.31	2.16	0.63	2.79	-0.11	[88]	
(NH <sub>2</sub> ) <sub>2</sub> bpy	Cl	MeTHF	3.44	2.16	0.63	2.79	0.02	[88]	
(isn) <sub>2</sub> bpy	Cl	MeTHF	3.22	2.00	0.49	2.49	0.25	[88]	
(OCH <sub>3</sub> ) <sub>2</sub> bpy	Cl	MeTHF	3.31	1.97	0.54	2.51	0.25	[88]	
dmb	Cl	MeTHF	3.22	1.98	0.52	2.50	0.20	[88]	
bpy	Cl	MeTHF	3.10	1.93	0.44	2.25	0.54	[88]	
Ph <sub>2</sub> bpy	Cl	MeTHF	3.02	1.92	0.44	2.36	0.22	[88]	
Cl <sub>2</sub> bpy	Cl	MeTHF	3.02	1.77	0.47	2.24	0.32	[88]	
(CO <sub>2</sub> Et) <sub>2</sub> bpy	Cl	MeTHF	2.88	1.73	0.37	2.11	0.40	[88]	
dmb	Etpy	DCE	3.48	2.30	<0.39	.41	2.70	0.41	[92]
bpy	Etpy	DCE	3.4	2.18	<0.48	.52	2.86	0.52	[92]

Cl <sub>2</sub> bpy	Etpy	DCE	2.15	<0.36	.31	2.73	0.31	[92]
CO <sub>2</sub> Me	Etpy	DCE	1.98	<0.34	.36	1.50	0.36	[92]

<sup>a</sup> Calculated from the BES spherical model. <sup>b</sup>  $\lambda_i = 0.22$  eV<sup>[90]</sup>.

The reduction potentials for either the oxidation ( $E_{1/2}^{+/*}$ ) or the reduction ( $E_{1/2}^{*/-}$ ) of the excited state can be calculated from the ground-state potential and the excited-state energy,  $E_{0,0}$  by

$$\begin{aligned}\Delta E_{1/2}^{*/-} &= E_{0,0} + \Delta E_{1/2}^{0/-} \\ \Delta E_{1/2}^{+/*} &= E_{0,0} - \Delta E_{1/2}^{0/+}\end{aligned}$$

The reduction potentials for the  $\text{Re}(\text{phen})(\text{CO})_3\text{Cl}^{+/*}\text{Re}(\text{phen})(\text{CO})_3\text{Cl}$  and  $^{*}\text{Re}(\text{phen})(\text{CO})_3\text{Cl}/\text{Re}(\text{phen})(\text{CO})_3\text{Cl}^{-}$  couples have been estimated<sup>[66]</sup> to be approximately  $-1.0$  and  $+1.0$  V (vs SCE in MeCN), respectively, using an excited-state energy of  $\approx 2.3$  eV. Using the estimates in Table 10 one obtains  $-1.2$  and  $+1.2$  V. The data in Tables 6 and 10 allow redox potentials for a number of other complexes to be calculated.

Visible light irradiation of a Re-alkyl complex,  $[\text{Re}(\alpha\text{-diimine})(\text{CO})_3\text{R}]$  ( $\text{R} = \text{CH}_3, \text{Et}, \text{iPr}, \text{or Bz}$ ;  $\text{dmb} = 4, 4'\text{-dimethyl-2,2' -bipyridine}$ ) gives rise to a homolytic cleavage of the Re-R bond with formation of the radicals  $[\text{Re}(\text{dmb})(\text{CO})_3]^{\bullet}$  and  $\text{R}^{\bullet}$ <sup>[73]</sup>. The reaction proceeds with a quantum efficiency of 0.4 for  $\text{R} = \text{CH}_3$  and 1 for  $\text{R} = \text{Et}, \text{iPr}, \text{or Bz}$ . The time-resolved UV-vis and IR absorption spectra reveal that for  $\text{Re}(\text{dmb})(\text{CO})_3(\text{CH}_3)$  the initially formed excited state is a  $^1\text{MLCT}$  state. The  $^1\text{MLCT}$  state can either pass over a thermal barrier of  $1560\text{ cm}^{-1}$  to the dissociative  $^3\sigma\pi^*$  state (and decompose into radicals) or decay nonradiatively to the  $^3\text{MLCT}$  state. In the case of  $\text{R} = \text{Et}, \text{iPr}, \text{or Bz}$ , the dissociative pathway to form the radical dominates. In all cases the radicals form in less than 10 ns.

### 2.2.3 Formate-rhenium complexes

*Fac*- $\text{Re}(\text{bpy})(\text{CO})_3\text{H}$  undergoes a thermally activated reaction with  $\text{CO}_2$  in organic solvents to produce the stable formate adduct, *fac*- $\text{Re}(\text{bpy})(\text{CO})_3(\text{O}_2\text{CH})$  <sup>[93]</sup>. The rate of formation is first order in  $[\text{CO}_2]$  and  $[\text{Re}]$  with a rate constant of  $2.0 \times 10^{-4}\text{ M}^{-1}\text{ s}^{-1}$  in THF and  $2.7 \times 10^{-2}\text{ M}^{-1}\text{ s}^{-1}$  in MeCN. Kinetic studies using *fac*- $\text{Re}(\text{bpy})(\text{CO})_3\text{D}$  reveals an inverse  $k_{\text{H}}/k_{\text{D}}$  isotope effect of  $\sim 0.5$  for both solvents. The reaction occurs by associative hydride-transfer.

While the thermal reaction is very slow at room temperature irradiation by 436 nm light increases the rate by more than a factor of 10<sup>[61]</sup>. While the CO<sub>2</sub> insertion into the Re-H bond reduces the CO<sub>2</sub>, the authors do not report CO or formate production. Nor is formate a product in photochemical CO<sub>2</sub> reduction systems that utilize *fac*-Re(bpy)(CO)<sub>3</sub>X<sup>[51-53, 72]</sup>, although the presence of Re(bpy)(CO)<sub>3</sub>(O<sub>2</sub>CH) was identified in such systems.

### 2.2.4 Re-CO<sub>2</sub> and Re-COOH complexes

Metallo-carboxylates and metallo-carboxylic acids are proposed as intermediates in photocatalytic reduction of CO<sub>2</sub> by *fac*-Re( $\alpha$ -diimine)(CO)<sub>3</sub>X, but have not been directly observed in the photocatalytic systems. Re(dmb)(CO)<sub>3</sub>(COOH), Re(bpy)(CO)<sub>3</sub>(CH<sub>2</sub>OH) and (CO)<sub>3</sub>(dmb)Re-C(O)-O-Re(dmb)(CO)<sub>3</sub> have been prepared by different routes and characterized<sup>[78, 79]</sup>. Reaction of Re(dmb)(CO)<sub>4</sub>(Otf) with aqueous KOH in water produces *fac*-Re(dmb)(CO)<sub>3</sub>(COOH) as a yellow precipitate. This complex has IR carboxylate absorptions,  $\nu_{\text{OCO}}$ , at 1572 and 1194 cm<sup>-1</sup>, which are at lower energy than those of the ruthenium analog, [Ru(bpy)<sub>2</sub>(CO)(COOH)]<sup>+</sup> (1618 and 1240 cm<sup>-1</sup>). The ruthenium complex has been prepared by a similar reaction (Ru(bpy)<sub>2</sub>(CO)<sub>2</sub><sup>2+</sup> with KOH) and characterized by x-ray crystal structure<sup>[94]</sup>. Reaction of Re(bpy)(CO)<sub>4</sub>(Otf) with NaBH<sub>4</sub> in methanol leads to the formation of the red Re(bpy)(CO)<sub>3</sub>(CH<sub>2</sub>OH). Irradiation of Re(bpy)(CO)<sub>3</sub>(CH<sub>2</sub>OH) in dry MeOH yields a red solid, *fac*-Re(bpy)(CO)<sub>3</sub>(OMe) in 97 % yield<sup>[78]</sup>. The authors suggest a  $\beta$ -elimination converts Re-CH<sub>2</sub>OH to Re-H, which upon photolysis reacts with MeOH to form Re-OMe.

The  $\mu^2$ - $\eta^2$ -CO<sub>2</sub>-bridged complex, (CO)<sub>3</sub>(dmb)Re-C(O)-O-Re(dmb)(CO)<sub>3</sub>, is isolated (together with several unidentified species) on standing from an acetone solution of *fac*-Re(dmb)(CO)<sub>3</sub>(COOH). Their IR data are summarized in Table 8. Neither *fac*-Re(dmb)(CO)<sub>3</sub>(O<sub>2</sub>CH) nor *fac*-Re(dmb)(CO)<sub>3</sub>(H) has been observed as a products in the decomposition of *fac*-Re(dmb)(CO)<sub>3</sub>(COOH)<sup>[79]</sup>. However *fac*-Re(dmb)(CO)<sub>3</sub>(COOH) with CO<sub>2</sub> in DMSO or DMF containing small amounts of water transforms to the bicarbonato complex, *fac*-Re(dmb)(CO)<sub>3</sub>(OC(O)OH) together with a small amount of the formato complex,

*fac*-Re(dmb)(CO)<sub>3</sub>(O<sub>2</sub>CH)<sup>[95]</sup>. The detail mechanisms involving these species need to be elucidated.

### 2.3. Electrochemical studies: One-electron and two-electron pathways

Extensive electrochemical studies on *fac*-Re(bpy)(CO)<sub>3</sub>Cl in MeCN, THF or DMF indicate that reduction of *fac*-Re(bpy)(CO)<sub>3</sub>Cl gives the radical anion, Re(bpy)(CO)<sub>3</sub>Cl<sup>•-</sup>, which reacts with CO<sub>2</sub> after loss of chloride. As shown in Figure 8, CO<sub>2</sub> reduction is proposed<sup>[49, 56, 58]</sup> to occur by two independent routes, a 1e pathway via Re(bpy)(CO)<sub>3</sub><sup>•</sup> and a 2e pathway via Re(bpy)(CO)<sub>3</sub><sup>-</sup>. FTIR studies of Re(bpy)(CO)<sub>3</sub>Cl<sup>•-</sup> (ν<sub>co</sub> 2012, 1903, 1882 cm<sup>-1</sup>) indicate that it is in equilibrium with Re(bpy)(CO)<sub>3</sub>(solvent)<sup>•</sup> (ν<sub>co</sub> 2015, 1902 cm<sup>-1</sup>) and [Re(bpy)(CO)<sub>3</sub>]<sub>2</sub> (ν<sub>co</sub> 1988, 1951, 1887, 1859 cm<sup>-1</sup>) in THF and MeCN. Unfortunately, the equilibrium constants and the rate constant for Cl<sup>-</sup> loss from Re(bpy)(CO)<sub>3</sub>Cl<sup>•-</sup> have not been determined. Reduction of Re(bpy)(CO)<sub>3</sub>(MeCN)<sup>+</sup> in THF leads to formation of three species: Re(bpy)(CO)<sub>3</sub>(MeCN)<sup>•</sup>, Re(bpy)(CO)<sub>3</sub>(THF)<sup>+</sup>, and [Re(bpy)(CO)<sub>3</sub>]<sub>2</sub>. Re(bpy)(CO)<sub>3</sub>(THF)<sup>•</sup> is not observed even in the reduction of Re(bpy)(CO)<sub>3</sub>(Otf) in THF. Thus Re(bpy)(CO)<sub>3</sub>(THF)<sup>•</sup> is unstable and rapidly dimerizes after loss of THF.

IR spectral changes during the further reduction of Re(bpy)(CO)<sub>3</sub>Cl<sup>•-</sup> indicate rapid loss of a Cl<sup>-</sup> ligand with formation of [Re(bpy)(CO)<sub>3</sub>]<sup>-</sup>. The further reduction of either [Re(bpy)(CO)<sub>3</sub>(solvent)]<sup>•</sup> or [Re(bpy)(CO)<sub>3</sub>]<sub>2</sub> also yields [Re(bpy)(CO)<sub>3</sub>]<sup>-</sup>. This illustrates the instability of non π-backbonding ligands coordinated to the formally Re<sup>0</sup> center.

IR spectral changes of Re(bpy)(CO)<sub>3</sub>Cl (with excess Cl<sup>-</sup>) or Re(bpy)(CO)<sub>3</sub>(Otf) (without excess Cl<sup>-</sup>) in electrochemical reduction in THF under CO<sub>2</sub> atmosphere indicate the disappearance of Re(bpy)(CO)<sub>3</sub>X (X = Cl or Otf) and the formation of [Re(bpy)(CO)<sub>3</sub>(O<sub>2</sub>CH)]<sup>-</sup> (ν<sub>COO</sub> 1628 cm<sup>-1</sup>), CO<sub>3</sub><sup>2-</sup> (ν<sub>COO</sub> 1643 cm<sup>-1</sup>), CO and an unidentified species with ν<sub>COO</sub> at 1680 cm<sup>-1</sup> (carboxylate?)<sup>[56]</sup>. It is reported that the ν<sub>COO</sub> band of Re(bpy)(CO)<sub>3</sub>(O<sub>2</sub>CH) and [Re(bpy)(CO)<sub>3</sub>(O<sub>2</sub>CH)]<sup>-</sup> are coincident (See Table 8). IR spectral changes of Re(bpy)(CO)<sub>3</sub>Cl in MeCN with excess Cl<sup>-</sup> under a CO<sub>2</sub> atmosphere have been reported to illustrate rapid

formation of free  $\text{CO}_3^{2-}$  ( $\nu_{\text{COO}}$  1643  $\text{cm}^{-1}$ ) and CO, together with an unassigned product having  $\nu_{\text{COO}}$  at 1679  $\text{cm}^{-1}$ . The unassigned product appears before formation of  $\text{CO}_3^{2-}$ . The IR spectrum in the  $\nu_{\text{CO}}$  region shows only small amounts of  $[\text{Re}(\text{bpy})(\text{CO})_3\text{Cl}]^{*-}$  and  $[\text{Re}(\text{bpy})(\text{CO})_3(\text{MeCN})]^*$  compared to the parent  $\text{Re}(\text{bpy})(\text{CO})_3\text{Cl}$  and free  $\text{CO}_3^{2-}$ , indicative of the catalytic nature of  $\text{CO}_3^{2-}$  production. Both  $[\text{Re}(\text{bpy})(\text{CO})_3]^*$  (1e pathway) and  $[\text{Re}(\text{bpy})(\text{CO})_3]^-$  (2e pathway) are alleged to react with  $\text{CO}_2$ .

The authors suggest a modification of the original mechanism show in Figure 8. In this mechanism, shown in Figure 9, the actual catalytic species is  $\text{Re}(\text{bpy})(\text{CO})_3\text{S}^*$  i.e., the one-electron reduced species that has had X replaced by a solvent molecule. This species is formed from the original  $\text{Re}(\text{bpy})(\text{CO})_3\text{X}^{n+}$  upon one-electron reduction. It is asserted that the electron density on the Re center is of critical importance in the catalytic scheme. The Re center must be sufficiently electronically poor to allow coordination of Lewis bases such as phosphines or MeCN otherwise rapid dimerization will occur. The use of a slightly coordinating solvent or free  $\text{Cl}^-$  in solution helps to suppress this reaction. Alternatively, the Re center must be electronically rich enough to coordinate and reduce  $\text{CO}_2$ .

The main products observed, CO and  $\text{CO}_3^{2-}$ , are produced by both pathways. The authors assert<sup>[56]</sup> that production of the major side product  $\text{Re}(\text{bpy})(\text{CO})_3(\text{O}_2\text{CH})$  ( $\nu_{\text{COO}}$  1630  $\text{cm}^{-1}$ ) is suppressed when the two-electron pathway dominates as it does when using  $[\text{Re}(\text{bpy})(\text{CO})_3\{\text{P}(\text{OEt})_3\}]^+$  or  $\text{Re}(\text{bpy})(\text{CO})_3\text{Cl}$  in MeCN. They assume that  $\text{Re}(\text{bpy})(\text{CO})_3(\text{O}_2\text{CH})$  is produced from either  $[\text{Re}(\text{bpy})(\text{CO})_3(\text{CO}_2)]^*$  or  $[\text{Re}(\text{bpy})(\text{CO})_3(\text{CO}_2)]^-$  by addition of  $e^-$  and  $\text{H}^+$  or  $\text{H}^+$ , respectively. However, such transformations to metal-formate complexes are not well characterized. Rhenium carboxylates ( $[\text{Re}(\text{bpy})(\text{CO})_3(\text{COO})]$  and  $[\text{Re}(\text{bpy})(\text{CO})_3(\text{COO})]^-$ ) are generally proposed<sup>[96]</sup> as intermediates in the electrochemical reduction of  $\text{CO}_2$  to CO (and  $\text{CO}_3^{2-}$ ) but no direct spectroscopic evidence has been obtained except for the IR absorption,  $\nu_{\text{COO}}$ , at 1680  $\text{cm}^{-1}$  for an unidentified species. Reported IR spectra involving this unidentified species show a relatively intense  $\nu_{\text{COO}}$  band compared to the of  $\nu_{\text{CO}}$

bands. Normally, the molar absorptivity of the  $\nu_{\text{CO}}$  band for bound CO is typically 3-5 times larger than that for bound  $\text{CO}_2$ [26, 97, 98]. The correct identification of this species is essential.

Table 11. Photocatalytic Reduction of CO<sub>2</sub> with Re(bpy)(CO)<sub>3</sub>X in DMF with TEOA as an electron donor.

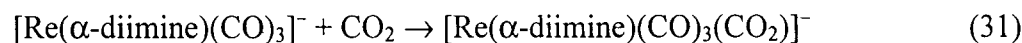
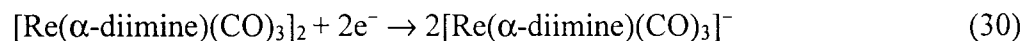
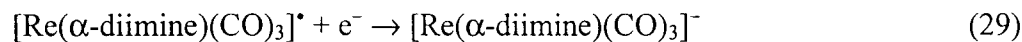
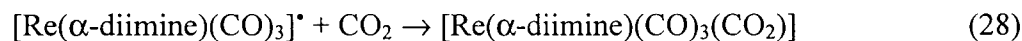
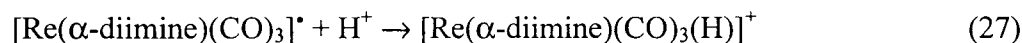
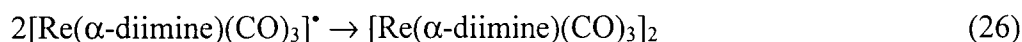
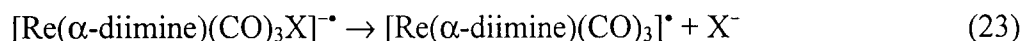
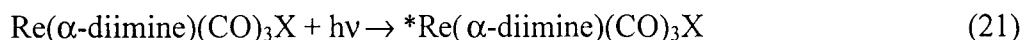
Sensitizer	Additives	Product	$\Phi^b$ , mol einstein <sup>-1</sup>	Ref.
Re(bpy)(CO) <sub>3</sub> Cl	Cl <sup>-</sup>	CO	0.14	[50, 51]
Re(bpy)(CO) <sub>3</sub> Br		CO	0.13	[52, 53]
Re(bpy)(CO) <sub>3</sub> Br	10 % H <sub>2</sub> O	CO	0.079	[53]
Re(bpy)(CO) <sub>3</sub> Br	20 % EtOH	CO	0.11	[53]
Re(bpy)(CO) <sub>3</sub> Br	Br <sup>-</sup>	CO	0.14	[53]
Re(bpy)(CO) <sub>3</sub> P(OEt) <sub>3</sub> <sup>+</sup>		CO	0.38	[54]
Re(bpy)(CO) <sub>3</sub> P(OEt) <sub>3</sub> <sup>+</sup>		CO	0.16	[67]
Re(bpy)(CO) <sub>2</sub> {P(OEt) <sub>3</sub> } <sub>2</sub> <sup>+</sup>		CO		[64]
Re(bpy)(CO) <sub>3</sub> (PPh <sub>3</sub> ) <sup>+</sup>		CO	0.05	[72]
Re(bpy)(CO) <sub>3</sub> (PEt <sub>3</sub> ) <sup>+</sup>		CO	0.024	[67]
Re(bpy)(CO) <sub>3</sub> {P(n-Bu) <sub>3</sub> } <sup>+</sup>		CO	0.013	[67]
Re(bpy)(CO) <sub>3</sub> {P(O-i-Pr) <sub>3</sub> } <sup>+</sup>		CO	0.20	[67]
Re(bpy)(CO) <sub>3</sub> P(OMe) <sub>3</sub> <sup>+</sup>		CO	0.17	[67]
Re(dmb)(CO) <sub>3</sub> P(OEt) <sub>3</sub> <sup>+</sup>		CO	0.18	[67]
Re{(CF <sub>3</sub> ) <sub>2</sub> bpy}(CO) <sub>3</sub> P(OEt) <sub>3</sub> <sup>+</sup>		CO	0.005	[67]

#### 2.4. Photochemical CO<sub>2</sub> reduction with Re( $\alpha$ -diimine)(CO)<sub>3</sub>X and Re( $\alpha$ -diimine)(CO)<sub>2</sub>XX'

Re( $\alpha$ -diimine)(CO)<sub>3</sub>X (X = halide, solvent, monodentate phosphine ligand, etc.) has been used as a photocatalyst for CO<sub>2</sub> reduction with TEOA in DMF [50-54, 67, 72] (Table 11). The <sup>3</sup>MLCT excited states of these Re complexes are reductively quenched by TEOA (TEOA<sup>+•/0</sup> potential  $\approx$  0.8 V) [47] to form [Re<sup>I</sup>(bpy<sup>-</sup>)(CO)<sub>3</sub>X]<sup>•</sup>. Transient spectroscopy show the expected

bpy<sup>-</sup> radical UV-vis absorption and ESR signals. When X = Br<sup>-</sup>, Cl<sup>-</sup>, or P(OEt<sub>3</sub>), the quenching rate constants are  $6 \times 10^7 \text{ M}^{-1} \text{ s}^{-1}$  [52],  $8 \times 10^7 \text{ M}^{-1} \text{ s}^{-1}$  [60], and  $1.1 \times 10^9 \text{ M}^{-1} \text{ s}^{-1}$  [67], respectively, in MeCN or DMF. Transient IR spectra of both the <sup>3</sup>MLCT excited state and the radical anion for Re(bpy)(CO)<sub>3</sub>Cl [76], Re(4,4'-bpy)<sub>2</sub>(CO)<sub>3</sub>Cl [75], Re(4,4'-bpy)<sub>2</sub>(CO)<sub>3</sub>(MeCN)<sup>+</sup> [74], Re(bpy)(CO)<sub>2</sub>{P(OEt)<sub>3</sub>}<sub>2</sub><sup>+</sup> [64], Re(bpy)(CO)<sub>3</sub>(MeCN)<sup>+</sup> [80],[74], Re(dmb)(CO)<sub>3</sub>(MeCN)<sup>+</sup> [74], and Re(dmb)(CO)<sub>3</sub>(CH<sub>3</sub>) [73] have been measured. Transient IR shows the expected shifts of ν<sub>CO</sub> for both the excited state to higher (20-80 cm<sup>-1</sup>) and the reduced species to lower energy (-15 to -40 cm<sup>-1</sup>)[69, 74-76] (see Table 8). Interestingly a small amount of doubly reduced [Re(dmb)(CO)<sub>3</sub>]<sup>-</sup> has been observed in the flash photolysis of Re(dmb)(CO)<sub>3</sub>(MeCN)<sup>+</sup> in MeCN with TEA[74].

The subsequent reactions of the radical species depend on the nature of α-diimine, X, solvent, and electron donor as also found in the electrochemical studies. The mechanism for photochemical CO<sub>2</sub> reduction must account for reactions of the electron donor (e.g., TEOA or TEA) and its reaction products. TEOA or TEA can coordinate to metal complexes and change their redox properties[21]. The following reactions can all become important under different conditions.



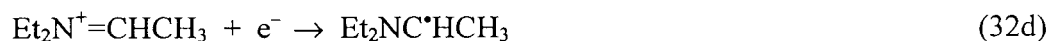
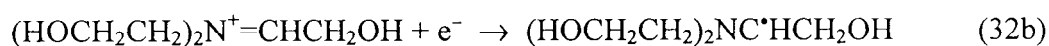
Both electrochemical and photochemical reduction of  $\text{Re}(\text{bpy})(\text{CO})_3\text{X}$  ( $\text{X} = \text{halide}$ ), yield  $[\text{Re}(\text{bpy})(\text{CO})_3\text{Cl}]^-$  [49]. It has been suggested that  $[\text{Re}(\text{bpy})(\text{CO})_3\text{Cl}]^-$  reacts directly with  $\text{CO}_2$ ; however, electrochemical results [49, 56] indicate that  $\text{CO}_2$  attachment only takes place after loss of  $\text{Cl}^-$ . The labilization of  $\text{Cl}^-$  produces either a five-coordinate  $[\text{Re}(\text{bpy})(\text{CO})_3]^+$  or the six-coordinate  $[\text{Re}(\text{bpy})(\text{CO})_3\text{S}]^+$ . The five-coordinate species can dimerize but under photolysis conditions their low concentration makes this reaction slow. The intermediates may react with  $\text{CO}_2$  or pick up a second electron and a proton to give  $\text{Re}(\text{bpy})(\text{CO})_3\text{H}$ . The formation of  $\text{Re}(\text{bpy})(\text{CO})_3\text{H}$  and  $\text{Re}(\text{bpy})(\text{CO})_3(\text{O}_2\text{CH})$  have been reported for  $\text{Re}(\text{bpy})(\text{CO})_3\text{X}$  ( $\text{X} = \text{Cl}$  and  $\text{Br}$ ) systems [33, 49, 50, 52, 53, 61]. While formate complexes generally produce formate, metal carboxylates (or metal  $\text{CO}_2$  adducts) generally lead to  $\text{CO}$  production [96]. Hawecker et al [51] concluded that the  $\text{Re}(\text{bpy})(\text{CO})_3(\text{O}_2\text{CH})$  is a side-product and an unlikely intermediate in the photochemical  $\text{CO}$  production, since:  $\text{Re}(\text{bpy})(\text{CO})_3(\text{O}_2\text{CH})$  is less active as a  $\text{CO}_2$  photoreduction catalysts than  $\text{Re}(\text{bpy})(\text{CO})_3(\text{Cl})$ ; the system with  $\text{Re}(\text{bpy})(\text{CO})_3(\text{O}_2\text{CH})$  produces only a small amount of  $\text{H}_2$  without any  $\text{CO}$ ; and  $\text{Re}(\text{bpy})(\text{CO})_3(\text{O}_2\text{CH})$  production is suppressed in the presence of excess  $\text{Cl}^-$  whereas in the absence of excess  $\text{Cl}^-$  ion  $\text{Re}(\text{bpy})(\text{CO})_3(\text{O}_2\text{CH})$  accumulates. Also  $\text{Re}(\text{bpy})(\text{CO})_3(\text{O}_2\text{CH})$  is formed as a side-product in the electrochemical reduction [56].

$\text{Re}(\text{bpy})(\text{CO})_3\{\text{P}(\text{OEt})_3\}^+$  produces  $\text{CO}$  with the highest quantum yield of up to 0.38 [54]. The quantum yield and turnover number using  $\text{Re}(\text{bpy})(\text{CO})_3\{\text{P}(\text{OEt})_3\}^+$  depend on the intensity and wavelength of the exciting light; however, for  $\text{Re}(\text{bpy})(\text{CO})_3\text{Cl}$  neither quantum yield nor turnover number are intensity and wavelength dependent. Since the lifetime of  $[\text{Re}(\text{bpy})(\text{CO})_3\{\text{P}(\text{OEt})_3\}]^+$  (514 s) is much longer than that of  $[\text{Re}(\text{bpy})(\text{CO})_3\text{Cl}]^+$  (6 s) under Ar in DMF, an inner filter effect by  $[\text{Re}(\text{bpy})(\text{CO})_3\{\text{P}(\text{OEt})_3\}]^+$  may explain the wavelength and intensity dependence [54].

Electrochemical studies indicate that  $[\text{Re}(\text{bpy})(\text{CO})_3\{\text{P}(\text{OEt})_3\}]^+$  is very stable and does not lose  $\text{P}(\text{OEt})_3$  or react with  $\text{CO}_2$  in THF [56]. Only on further reduction does the complex lose  $\text{P}(\text{OEt})_3$  to form the five-coordinate anion  $[\text{Re}(\text{bpy})(\text{CO})_3]^-$  which can react with  $\text{CO}_2$ . The

first and second reduction potentials of  $\text{Re}(\text{bpy})(\text{CO})_3\{\text{P}(\text{OEt})_3\}^+$  are reported to be -1.25 and  $\approx$  -1.9 V vs SCE in MeCN<sup>[56, 62]</sup>, assuming the Fc/Fc<sup>+</sup> and Ag/AgNO<sub>3</sub> potentials are 0.38 V and 0.33 V vs SCE, respectively. The  $E_{0-0}$  of the <sup>3</sup>MLCT state of the  $\text{Re}(\text{bpy})(\text{CO})_3\{\text{P}(\text{OEt})_3\}^+$  is  $\approx$  2.8 eV (Table 10) thus the excited-state reduction potential is  $\approx$  1.5 V ( $E_{1/2}^{+/0} = -1.25$  V vs SCE) thus the quenching of the  $^*\text{Re}(\text{bpy})(\text{CO})_3\{\text{P}(\text{OEt})_3\}^+$  by TEOA ( $E_{1/2}^{+/0} = 0.6$  V vs SCE<sup>[99]</sup>) has a  $\Delta E^0 \approx 0.9 = (1.5 - 0.6)$  V.

The TEOA<sup>•+</sup> radical,  $(\text{HOCH}_2\text{CH}_2)_3\text{N}^{\bullet+}$ , can react with another TEOA to form the carbon radical  $(\text{HOCH}_2\text{CH}_2)_2\text{NC}^*\text{HCH}_2\text{OH}$  as shown in Eq 32a.



While  $(\text{HOCH}_2\text{CH}_2)_2\text{NC}^*\text{HCH}_2\text{OH}$  is known to be a strong reducing agent its potential is not known. The reduction potentials of TEA<sup>•+</sup> and TEOA<sup>•+</sup> are 0.96<sup>[100]</sup> and 0.6 V<sup>[99]</sup> vs SCE in MeCN, respectively. Thus TEOA, with its electronegative oxygens, is a better reducing agent than TEA. The reduction potential of  $\text{Et}_2\text{N}^+=\text{CHCH}_3$  (of Eq. 32d) has been measured to be -1.12 V vs SCE in MeCN, <sup>[101]</sup> so the potential of  $(\text{HOCH}_2\text{CH}_2)_2\text{N}^+=\text{CHCH}_2\text{OH}$  (of Eq. 32b) will be more negative than -1.12 V. Thus while  $(\text{HOCH}_2\text{CH}_2)_2\text{N}^+=\text{CHCH}_2\text{OH}$  may reduce  $\text{Re}(\text{bpy})(\text{CO})_3\text{Cl}$  ( $E_{1/2} = -1.35$  V) and  $[\text{Re}(\text{bpy})(\text{CO})_3\{\text{P}(\text{OEt})_3\}]^+$  ( $E_{1/2} = -1.25$  V), it is not expected to reduce  $[\text{Re}(\text{bpy})(\text{CO})_3\text{Cl}]^*$  ( $E_{1/2} \sim -1.7$  V) or  $[\text{Re}(\text{bpy})(\text{CO})_3\{\text{P}(\text{OEt})_3\}]^*$  ( $E_{1/2} \sim -1.9$  V). The above suggests that while the doubly reduced  $[\text{Re}(\text{bpy})(\text{CO})_3\{\text{P}(\text{OEt})_3\}]^-$  is formed in the electrochemical system the formation is not possible in the photochemical system. Since the  $[\text{Re}(\text{bpy})(\text{CO})_3\{\text{P}(\text{OEt})_3\}]^*$  does not lose  $\text{P}(\text{OEt})_3$ <sup>[54]</sup>, it is hard to understand how the singly reduced Re complex can acquire a CO<sub>2</sub> ligand.

Koike et al. assume that the monoreduced  $[\text{Re}(\text{bpy})(\text{CO})_3(\text{PR}_3)]^*$  reacts with CO<sub>2</sub> or dimerizes in the photochemical system they studied<sup>[67]</sup>. From the decay of  $[\text{Re}(\text{bpy})(\text{CO})_3(\text{PR}_3)]^*$  observed during continuous photolysis under CO<sub>2</sub>, the CO<sub>2</sub> binding rates

constants have been estimated:  $\text{Re}(\text{bpy})(\text{CO})_3\{\text{P}(\text{OEt})_3\}$ :  $8.8 \times 10^{-3} \text{ M}^{-1} \text{ s}^{-1}$  [54];  $\text{Re}(\text{bpy})(\text{CO})_3\{\text{P}(\text{OEt})_3\}$ :  $5.6 \times 10^{-3} \text{ M}^{-1} \text{ s}^{-1}$  [67];  $\text{Re}(\text{bpy})(\text{CO})_3\{\text{P}(\text{O-}i\text{-Pr})_3\}$ :  $9.4 \times 10^{-3} \text{ M}^{-1} \text{ s}^{-1}$  [67];  $\text{Re}(\text{dmb})(\text{CO})_3\{\text{P}(\text{OEt})_3\}$ :  $18.6 \times 10^{-3} \text{ M}^{-1} \text{ s}^{-1}$  [67]. These  $\text{CO}_2$  binding rate constants are very slow compared to those of other metal complexes that act as photocatalysts: ( $\text{CoHMD}^+$ :  $1.8 \times 10^8 \text{ M}^{-1} \text{ s}^{-1}$  [22],  $\text{Ni}(\text{cyclam})^+$ :  $3.2 \times 10^7 \text{ M}^{-1} \text{ s}^{-1}$  [18],  $\text{Pd}(\text{etpC})(\text{DMF})^+$ :  $53 \text{ M}^{-1} \text{ s}^{-1}$  [102]) The authors did not detect formation of either the Re dimer or the  $\text{CO}_2$  complex. Since they did not measure the dependence of the  $\text{CO}_2$  binding rate on Re or  $\text{CO}_2$  concentration, the actual pathway in the photochemical system is probably more complicated. Thus of fundamental importance in understanding photochemical  $\text{CO}_2$  fixation is the elucidation of the mechanism that allows the singly reduced Re complex to bind  $\text{CO}_2$ . One interesting possibility is that the reduced Re complex is photolabile and that the absorption of a second photon assists the loss of the sixth ligand. Detailed studies of the  $\text{Re}(\text{bpy})(\text{CO})_3\text{X}$  ( $\text{X} = \text{Cl}$  and  $\text{Br}$ ) photochemical systems that report formation of  $\text{Re}(\text{bpy})(\text{CO})_3\text{H}$ ,  $\text{Re}(\text{bpy})(\text{CO})_3(\text{O}_2\text{CH})$  and  $\text{Re}(\text{Mebpy})(\text{CO})_3\text{Br}$  in addition to the dimer [33, 49, 50, 52, 53, 61, 103] are needed.

### 3. Conclusions

Nonbiological artificial photosynthetic systems offer the possibility of producing fuels and chemicals from  $\text{CO}_2$  and sunlight in fewer steps and with higher efficiencies than in natural systems. It may also be possible to design such systems to operate under conditions and in environments where plant growth is not optimal or practical. Light capture, electron transfer, and catalysis must be coupled efficiently. However, the approaches described in this chapter have several problems. All the systems require a sacrificial reagent. The stability of the systems is limited, the catalytic activities are too low, and the overall costs are too high for commercialization. Dark reactions including the bond formation and cleavage steps are relatively slow. It is very important to investigate the factors controlling reaction rates and efficiencies through kinetic and mechanistic studies. At this stage, many questions remain. Hopefully, the insight obtained from a fundamental understanding of the reactions occurring in

the above systems will provide the knowledge for the design of practical systems. One fundamental and formidable challenge is the replacement of the “sacrificial” electron donors by species that will lead to useful (or benign) chemicals in their own right.

**Acknowledgement.** We thank Drs. Norman Sutin and David Thompson (BNL) and Prof. Osamu Ishitani (Saitama University, Japan) for their helpful comments, and Prof. Shoichi Kita (Hirosaki University, Japan) for providing his unpublished data obtained during his stay at BNL. Brookhaven National Laboratory is funded under contract DE-AC02-98CH10886 with the U.S. Department of Energy and supported by its Division of Chemical Sciences, Office of Basic Energy Sciences.

Appendix A Abbreviations

Abbreviation	Chemical Name
bcyclam	6,6'-bis(1,4,8,11-tetraazacyclotetradecane
bMe <sub>2</sub> cyclam	6,6'-bis(5,7-dimethyl-1,4,8,11-tetraazacyclotetradecane)
4,4'-bpy	4,4'-bipyridine
bpy	2,2'-bipyridine
bpz	2,2'-bipyrazine
Brphen	5-bromo-1,10-phenanthroline
Cl <sub>2</sub> bpy	4,4'-dichloro-2,2'-bipyridine
Clphen	5-chloro-1,10-phenanthroline
(CO <sub>2</sub> Et) <sub>2</sub> bpy	4,4'-bis(ethoxycarbonyl)-2,2'-bipyridine
cyclam	1,4,8,11-tetraazacyclotetradecane
DCE	1,2-dichloroethane
dmb	4,4'-dimethyl-2,2'-bipyridine
DMD	5,12-dimethyl-1,4,8,11-tetraazacyclotetradeca-4,11-diene
DMF	N,N-dimethylformamide
DMSO	dimethylsulfoxide
dpp	2,3-di(2-pyridyl)pyrazine
dpq	2,3-di(2-pyridyl)quinoxaline
EtCN	propionitrile
EtOH	ethanol
etpC	bis[(dicyclohexylphosphino)ethyl]phenylphosphine
4Etpy	4-ethylpyridine
H <sub>2</sub> A	ascorbic acid
HMD	5,7,7,12,14,14-hexamethyl-1,4,8,11-tetraazacyclotetradeca-4,11-diene
3HOpy	3-hydroxypyridine
HTIM	2,3,9,10-tetramethyl-1,4,8,11-tetraazacyclotetradecane
(isn) <sub>2</sub> bpy	4,4'-isonitrile-2,2'-bipyridine
Me <sub>2</sub> cyclam	5,7-dimethyl-1,4,8,11-tetraazacyclotetradecane
Mebpy	5-methyl-2,2'-bipyridine
MeCN	acetonitrile
Meimz	N-methylimidazole
MeOH	methanol
Mephen	5-methyl-1,10-phenanthroline
2Mepy	2-methylpyridine
3Mepy	3-methylpyridine
4Mepy	4 methylpyridine

MeTHF	2-methyltetrahydrofuran
MV <sup>2+</sup>	methylviologen
(NEt <sub>2</sub> ) <sub>2</sub> bpy	4,4'-di(N,N-diethylamino)-2,2'-bipyridine
(NH <sub>2</sub> ) <sub>2</sub> bpy	4,4'-diamino-2,2'-bipyridine
(OCH <sub>3</sub> ) <sub>2</sub> bpy	4,4'-dimethoxy-2,2'-bipyridine
OMD	3,5,7,7,10,12,14,14-octamethyl-1,4,8,11-tetraazacyclotetradeca-4,11-diene
Otf	trifluoromethanesulfonate
Ph <sub>2</sub> bpy	4,4'-diphenyl-2,2'-bipyridine
Ph <sub>2</sub> phen	4,7-diphenyl-1,10-phenanthroline
phen	1,10-phenanthroline
Phena	phenazine
4Phpy	4-phenylpyridine
PrCN	butyronitrile
Pr-cyclam	6-((N- <i>p</i> -methoxybenzyl)pyridin-4-yl)methyl-1,4,8,11-tetraazacyclotetradecane or 6-((N-benzyl)pyridin-4-yl)methyl-1,4,8,11-tetraazacyclotetradecane
py	pyridine
TEA	triethylamine
TEOA	triethanolamine
THF	tetrahydrofuran
TP	<i>p</i> -terphenyl

---

### Techniques

---

$E_{1/2}$	half-cell potential
$E_{pa}$	peak potential of the anodic scan
$E_{pc}$	peak potential of the cathodic scan
EXAFS	extended X-ray absorption fine structure
FTIR	Fourier-Transform Infrared
NHE	normal hydrogen electrode
SCE	saturated calomel electrode
SSCE	Sodium-saturated calomel electrode
XANES	X-ray absorption near-edge spectroscopy

---

## Figure Captions

- Fig. 1 Schematic diagram of artificial photosynthesis.
- Fig. 2 Structures and geometries of metal macrocycles.
- Fig. 3 Four  $\text{CoHMD}(\text{CO}_2)^+$  species observed in a  $\text{CD}_3\text{CN}/\text{THF}$  mixture by FTIR.
- Fig. 4 XANES for a series of CoHMD complexes in various oxidation and ligation states. (a)  $[\text{Co}^{\text{II}}\text{HMD}](\text{ClO}_4)_2$  in acetonitrile at 150 K (—),  $[\text{Co}^{\text{III}}\text{HMD}(\text{CO}_3^{2-})]\text{ClO}_4$  in  $\text{H}_2\text{O}$  at room temperature (- - -), and  $[\text{Co}^{\text{I}}\text{HMD}(\text{CO})]\text{ClO}_4$  in acetonitrile at room temperature (---). (b)  $[\text{Co}^{\text{II}}\text{HMD}](\text{ClO}_4)_2$  in acetonitrile at 150 K (—), five-coordinate  $[\text{CoHMD}(\text{CO}_2)]\text{ClO}_4$  in acetonitrile at room temperature (---), six-coordinate  $[\text{S-CoHMD}(\text{CO}_2)]\text{ClO}_4$  in acetonitrile at 150 K (-----).
- Fig. 5 Schematic reaction mechanism for photochemical  $\text{CO}_2$  reduction using TP and ML.
- Fig. 6 Top left: Decay of  $\text{TP}^{*-}$  monitored at 470 nm; Top right: Growth of  $\text{Co}^{\text{I}}\text{HMD}^+$  monitored at 670 nm; Bottom: Transient absorption spectrum of  $\text{Co}^{\text{I}}\text{HMD}^+$  observed 6  $\mu\text{s}$  after the excitation for a degassed sample containing 0.1 mM TP, 0.5 M TEA, 0.1 M TEAP, and 1 mM  $\text{Co}^{\text{II}}\text{HMD}^{2+}$  in MeCN/MeOH.
- Fig. 7 Transient decay curve of  $\text{Co}^{\text{I}}\text{HMD}^+$  monitored at 670 nm for a sample containing 0.1 mM TP, 0.5 M TEA, 0.1 M TEAP, 1 mM  $\text{Co}^{\text{II}}\text{HMD}^{2+}$ , and 0.53 mM  $\text{CO}_2$  in MeCN/MeOH.
- Fig. 8 The relationship between  $E_{\text{abs}}$ ,  $E_{\text{em}}$ ,  $\lambda_{\text{re}}$ ,  $E_{\text{st}}$  and  $E_{0.0}$ .
- Fig. 9 One- and two-electron pathways for  $\text{CO}_2$  reduction: A = an oxide ion acceptor or  $\text{CO}_2$ .
- Fig. 10 Modified one- and two-electron pathways for  $\text{CO}_2$  reduction: S = solvent molecule.

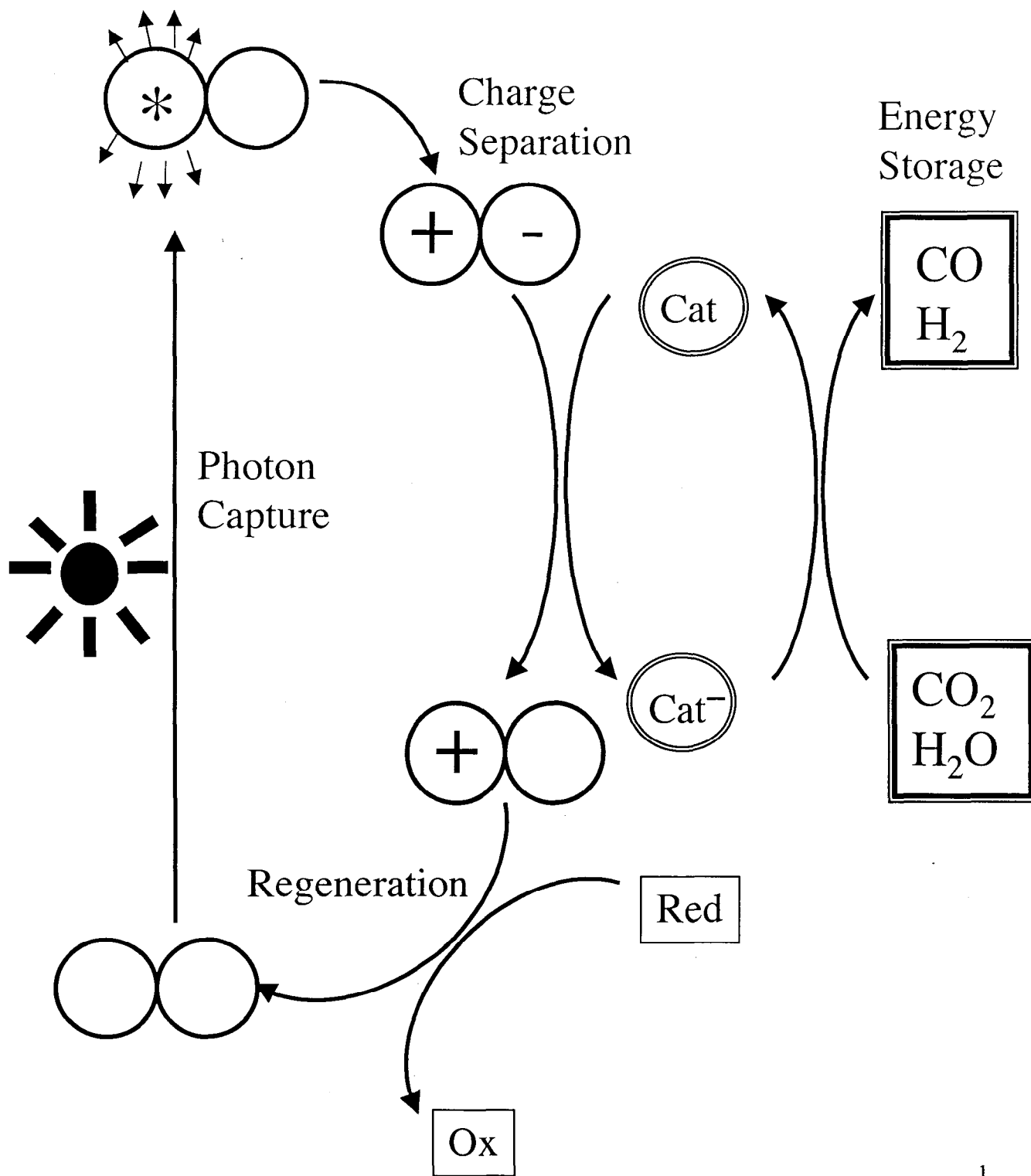
## References:

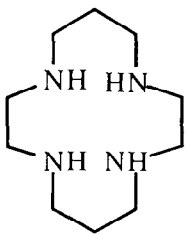
- [1] S. Sahami, M. J. Weaver, *Electroanal. Chem.* 122 (1981) 155-170.
- [2] S. Sahami, M. J. Weaver, *Electroanal. Chem.* 122 (1981) 171-181.
- [3] B. Fisher, R. Eisenberg, *J. Am. Chem. Soc.* 102 (1980) 7361-7365.
- [4] A. T. A. Tinnemans, T. P. M. Koster, D. H. M. W. Thewissen, A. Mackor, *Recl. Trav. Chim. Pays. -Bas* 103 (1984) 288-295.
- [5] M. Beley, J.-P. Collin, R. Ruppert, J.-P. Sauvage, *J. Chem. Soc., Chem. Commun.* (1984) 1315-1316.
- [6] M. Beley, J.-P. Collin, R. Ruppert, J.-P. Sauvage, *J. Am. Chem. Soc.* 108 (1986) 7461.
- [7] E. Fujita, J. Haff, R. Sanzenbacher, H. Elias, *Inorg. Chem.* 33 (1994) 4627-4628.
- [8] D. J. Szalda, C. L. Schwarz, J. F. Endicott, E. Fujita, C. Creutz, *Inorg. Chem.* 28 (1989) 3214-3219.
- [9] C. Creutz, H. A. Schwarz, J. F. Wishart, E. Fujita, N. Sutin, *J. Am. Chem. Soc.* 113 (1991) 3361-3371.
- [10] J. L. Grant, K. Goswami, L. O. Spreer, J. W. Otvos, M. Calvin, *J. Chem. Soc., Dalton Trans* (1987) 2105.
- [11] C. A. Craig, L. O. Spreer, J. W. Otvos, M. Calvin, *J. Phys. Chem.* 94 (1990) 7957.
- [12] S. Matsuoka, K. Yamamoto, T. Ogata, M. Kusaba, N. Nakashima, E. Fujita, S. Yanagida, *J. Am. Chem. Soc.* 115 (1993) 601-609.
- [13] D. J. Szalda, E. Fujita, C. Creutz, *Inorg. Chem.* 28 (1989) 1446.
- [14] E. Fujita, L. R. Furenlid, M. W. Renner, *J. Am. Chem. Soc.* 119 (1997) 4549-4550.
- [15] D. J. Szalda, E. Fujita, R. Sanzenbacher, H. Paulus, H. Elias, *Inorg. Chem.* 33 (1994) 5855-5863.
- [16] L. R. Furenlid, M. W. Renner, E. Fujita, *Physica B* 208 & 209 (1995) 739-742.
- [17] A. M. Tait, M. Z. Hoffman, E. Hayon, *Inorg. Chem.* 15 (1976) 934-939.
- [18] C. A. Kelly, Q. G. Mulazzani, M. Venturi, E. L. Blinn, M. A. Rodgers, *J. Am. Chem. Soc.* 117 (1995) 4911-4919.
- [19] D. Cabelli, (1999) .
- [20] A. M. Tait, M. Z. Hoffman, E. Hayon, *J. Am. Chem. Soc.* 98 (1976) 86.
- [21] E. Fujita, B. S. Brunshwig, D. Cabelli, M. W. Renner, L. R. Furenlid, T. Ogata, Y. Wada, S. Yanagida, *Photochemical carbon dioxide reduction with metal complexes: differences between cobalt and nickel macrocycles*, Elsevier, Amsterdam 1998.
- [22] T. Ogata, S. Yanagida, B. S. Brunshwig, E. Fujita, *J. Am. Chem. Soc.* 117 (1995) 6708-16.
- [23] G. M. Brown, B. S. Brunshwig, C. Creutz, J. F. Endicott, N. Sutin, *J. Am. Chem. Soc.* 101 (1979) 1298-1300.
- [24] D. A. Gangi, R. R. Durand, *J. Chem. Soc., Chem. Commun.* (1986) 697.
- [25] M. H. Schmidt, G. M. Miskelly, N. S. Lewis, *J. Am. Chem. Soc.* 112 (1990) 3420-3426.
- [26] E. Fujita, C. Creutz, N. Sutin, B. S. Brunshwig, *Inorg. Chem.* 32 (1993) 2657-2662.
- [27] E. Fujita, D. J. Szalda, C. Creutz, N. Sutin, *J. Am. Chem. Soc.* 110 (1988) 4870.
- [28] H. Tanaka, H. Nagao, S.-M. Peng, K. Tanaka, *Organometallics* 11 (1992) 1450-1451.
- [29] E. Fujita, C. Creutz, N. Sutin, D. J. Szalda, *J. Am. Chem. Soc.* 113 (1991) 343-353.
- [30] E. Fujita, R. van Eldik, *Inorg. Chem.* 37 (1998) 360-362.

- [31] S. Sakaki, A. Dedieu, *J. Organomet. Chem.* 314 (1986) C63.
- [32] S. Sakaki, A. Dedieu, *Inorg. Chem.* 26 (1987) 3278.
- [33] J. Hawecker, J.-M. Lehn, R. Ziessel, *J. Chem. Soc., Chem. Commun.* (1985) 56-58.
- [34] J.-M. Lehn, R. Ziessel, *J. Organometal. Chem.* 382 (1990) 157-173.
- [35] E. Kimura, S. Wada, M. Shionoya, T. Takahashi, Y. Iitaka, *J. Chem. Soc., Chem. Commun.* (1990) 397.
- [36] E. Kimura, X. Bu, M. Shionoya, S. Wada, S. Maruyama, *Inorg. Chem.* 31 (1992) 4542-4546.
- [37] E. Kimura, S. Wada, M. Shionoya, Y. Okazaki, *Inorg. Chem.* 33 (1994) 770-778.
- [38] E. Fujita, S. J. Milder, B. S. Brunschwig, *Inorg. Chem.* 31 (1992) 2079-2085.
- [39] K. Mochizuki, S. Manaka, I. Takeda, T. Kondo, *Inorg. Chem.* 35 (1996) 5132-5136.
- [40] E. Mejeritskaia, F. Luo, C. A. Kelly, B. Koch, E. M. Gundlach, E. L. Blinn, *Inorg. Chim. Acta* 246 (1996) 295-299.
- [41] S. Matsuoka, K. Yamamoto, C. Pac, S. Yanagida, *Chem. Lett.* (1991) 2099-2100.
- [42] T. Ogata, Y. Yamamoto, Y. Wada, K. Murakoshi, M. Kusaba, N. Nakashima, A. Ishida, S. Takamuku, S. Yanagida, *J. Phys. Chem.* 99 (1995) 11916-11922.
- [43] S. Matsuoka, T. Kohzuki, C. Pac, S. Yanagida, *Chemistry Letters* (1990) 2047.
- [44] S. Matsuoka, T. Kohzuki, C. Pac, A. Ishida, S. Takamuku, M. Kusaba, N. Nakashima, S. Yanagida, *J. Phys. Chem.* 96 (1992) 4437-4442.
- [45] J. Vasilevskis, D. C. Olson, *Inorg. Chem.* 10 (1971) 1228.
- [46] M. Wrighton, D. L. Morse, *J. Am. Chem. Soc.* 96 (1974) 998-1003.
- [47] K. Kalyanasundaram, J. Kiwi, M. Gratzel, *Helv. Chim. Acta* 61 (1978) 2720-2730.
- [48] D. J. Stufken, A. J. Vlcek, *Coord. Chem. Rev.* 177 (1998) 127-179.
- [49] B. P. Sullivan, C. M. Bolinger, D. Conrad, W. J. Vining, T. J. Meyer, *J. Chem. Soc. Chem. Commun.* (1985) 1414-1416.
- [50] J. Hawecker, J.-M. Lehn, R. Ziessel, *J. Chem. Soc., Chem. Commun.* (1983) 536-538.
- [51] J. Hawecker, J.-M. Lehn, R. Ziessel, *Helv. Chim. Acta* 69 (1986) 1990-2012.
- [52] C. Kutal, M. A. Weber, G. Ferraudi, D. Geiger, *Organometallics* 4 (1985) 2161-2166.
- [53] C. Kutal, A. J. Corbin, G. Ferraudi, *Organometallics* 6 (1987) 553-557.
- [54] H. Hori, F. P. A. Johnson, K. Koike, O. Ishitani, T. Ibusuki, *J. Photochem. Photobiol., A* 96 (1996) 171-174.
- [55] A. I. Breikss, H. D. Abruña, *J. Electroanal. Chem.* 201 (1986) 347-358.
- [56] F. P. A. Johnson, M. W. W. George, F. Hartl, J. J. Turner, *Organometallics* 15 (1996) 3374-3387.
- [57] G. J. Stor, F. Hartl, J. W. M. v. Outersterp, D. J. Stufkens, *Organometallics* 14 (1995) 1115-1131.
- [58] J. W. M. van Outersterp, F. Hartl, D. J. Stufkens, *Organometallics* 14 (1995) 3303-3310.
- [59] J. V. Caspar, T. J. Meyer, *J. Phys. Chem.* 87 (1983) 952-957.
- [60] K. Kalyanasundaram, *J. Chem. Soc., Faraday Trans.* 82 (1986) 2401-2415.
- [61] B. P. Sullivan, T. J. Meyer, *J. Chem. Soc., Chem. Commun.* (1984) 1224-1245.
- [62] O. Ishitani, 1999.
- [63] D. P. Summers, J. C. Luong, M. S. Wrighton, *J. Am. Chem. Soc.* 103 (1981) 5238-5241.
- [64] O. Ishitani, M. W. George, T. Ibusuki, F. P. A. Johnson, K. Koike, K. Nozaki, C. Pac, J. J. Turner, J. R. Westwell, *Inorg. Chem.* 33 (1994) 4712-4717.
- [65] P. Christensen, A. Hamnett, A. V. G. Muir, J. A. Timney, *J. Chem. Soc. Dalton Trans* (1992) 1455-1463.

- [66] J. C. Luong, L. Nadjó, M. S. Wrighton, *J. Am. Chem. Soc.* 100 (1978) 5790-5795.
- [67] K. Koike, H. Hori, M. Ishizuka, J. R. Westwell, K. Takeuchi, T. Ibusuki, K. Enjouji, H. Konno, K. Sakamoto, O. Ishitani, *Organometallics* 16 (1997) 5724-5729.
- [68] P. J. Giordano, M. S. Wrighton, *J. Am. Chem. Soc.* 101 (1979) 1067.
- [69] P. Glyn, M. W. George, P. M. Hodges, J. J. Turner, *J. Chem. Soc. Chem. Comm.* (1989) 1655-1657.
- [70] L. A. Lucia, R. D. Burton, K. S. Schanze, *Inorg. Chim. Acta.* (1993) 103-106.
- [71] B. Rossenaar, D. J. Stufkens, A. J. Vlcek, *Inorg. Chem.* 35 (1996) 2902-2909.
- [72] H. Hori, F. P. A. Johnson, K. Koike, K. Takeuchi, T. Ibusuki, O. Ishitani, *J. Chem. Soc., Dalton Trans.* (1997) 1019-1023.
- [73] C. J. Kleverlaan, D. J. Stufkens, I. P. Clark, M. W. George, J. J. Turner, D. M. Martino, H. van Willigen, A. J. Vlcek, *J. Am. Chem. Soc.* 120 (1998) 10871-10879.
- [74] S. Kita, B. S. Brunshwig, E. Fujita, (unpublished work) .
- [75] D. R. Gamelin, M. W. George, P. Glyn, F.-W. Grevels, F. P. A. Johnson, W. Klotzbucher, S. L. Morrison, G. Russell, K. Schaffner, J. J. Turner, *Inorg. Chem.* 33 (1994) 3246-3250.
- [76] M. W. George, F. P. A. Johnson, J. R. Westwell, P. M. Hodges, J. J. Turner, *J. Chem. Soc. Dalton Trans* (1993) 2977-2979.
- [77] C.-F. Shu, M. S. Wrighton, *Inorg. Chem.* 27 (1988) 4326-4329.
- [78] D. H. Gibson, B. A. Sleadd, X. Yin, *Organometallics* 17 (1998) 2689-2691.
- [79] D. H. Gibson, X. Yin, *J. Am. Chem. Soc.* 120 (1998) 11200-11201.
- [80] M. W. George, J. J. Turner, *Coord. Chem. Rev.* 177 (1998) 201.
- [81] I. P. Clark, M. W. George, F. P. A. Johnson, J. J. Turner, *J. Chem. Soc., Chem. Commun.* (1996) 1587-1588.
- [82] For the complexes considered here we expect that the nuclear configuration of the singlet and triplet MLCT states to be similar. Thus the Stokes shift between the two states is small.
- [83] The singlet-triplet and ground-excited state energy difference and the absorption and emission energies are treated as unsigned quantities and taken as positive.
- [84] B. S. Brunshwig, S. Ehrenson, N. Sutin, *J. Phys. Chem* 90 (1986) 3657-3668.
- [85] The spherical cavity model requires parameters for the solvent and the cavity to calculate the reorganization energy. The dimensions of the molecule have been obtained from models created in MacSparten. The cavity radius was calculated as  $r = \left( \sqrt[3]{d_1 d_2 d_3} \right) / 2$  where  $d_i$  are the three principle diameters of the molecule (including van der Waals end radius for each atom) and are 7.8, 11.26 and 11.26 respectively, with  $r = 5.0 \text{ \AA}$ . The Re atom is placed off center by  $1.3 \text{ \AA}$  and the electron transfer distance is  $3.5 \text{ \AA}$ . The optical (square of the refractive index) and static dielectric constants of the solvent have been used.
- [86] E. M. Kober, J. V. Caspar, R. S. Lumpkin, T. J. Meyer, *J. Phys. Chem.* 90 (1986) 3722.
- [87] J. V. Caspar, T. J. Meyer, *Inorg. Chem.* 22 (1983) 2444.
- [88] L. A. Worl, R. Duesing, P.-Y. Chen, L. D. Ciana, T. J. Meyer, *J. Chem. Soc.* (1991) 849-858.
- [89] L. Sacksteder, A. P. Zipp, E. A. Brown, J. Streich, J. N. Demas, B. A. DeGraff, *Inorg. Chem.* 29 (1990) 4335-4340.
- [90] J. P. Claude, T. J. Meyer, *J. Phys. Chem.* 99 (1995) 51-54.
- [91] J. A. Baiano, R. J. Kessler, R. S. Lumpkin, M. J. Munley, J. W. R. Murphy, *J. Phys. Chem.* (1995) .

- [92] P. Chen, R. Duesing, D. K. Graff, T. J. Meyer, *J. Phys. chem.* 95 (1991) 5850-5858.
- [93] B. P. Sullivan, T. J. Meyer, *Organometallics* 5 (1986) 1500- 1502.
- [94] K. Toyohara, H. Nagao, T. Adachi, T. Yoshida, K. Tanaka, *Chem. Lett.* (1996) 27-28.
- [95] D. H. Gibson, X. Yin, *J. Chem. Soc., Chem. Commun.* (1999) 1411-1412.
- [96] N. Sutin, C. Creutz, E. Fujita, *Comments Inorg. Chem.* 19 (1997) 67-92.
- [97] H. Tanaka, B.-C. Tzeng, H. Nagao, S.-M. Peng, K. Tanaka, *Inorg. Chem.* 32 (1993) 1508-1512.
- [98] J. R. Pinkes, C. J. Masi, R. Chiulli, B. D. Steffey, A. R. Cutler, *Inorg. Chem.* 36 (1997) 70-79.
- [99] H. Sun, M. Z. Hoffman, *J. Phys. Chem.* 98 (1994) 11719-11726.
- [100] J. W. Arbogast, C. S. Foote, M. Kao, *J. Am. Chem. Soc.* 114 (1992) 2277-2279.
- [101] D. D. M. Wayner, D. J. McPhee, D. Griller, *J. Am. Chem. Soc.* 110 (1988) 132-137.
- [102] D. L. DuBois, A. Miedaner, R. C. Haltiwanger, *J. Am. Chem. Soc.* 113 (1991) 8753-8764.
- [103] O. Ishitani, I. Namura, S. Yanagida, P. C., *J. Chem. Soc., Chem. Commun.* (1987) 1153-1154.

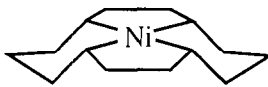




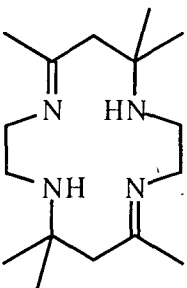
cyclam



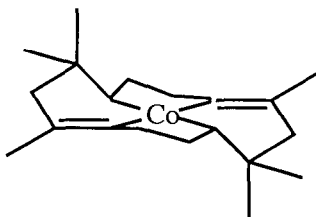
cyclam, *Trans III*



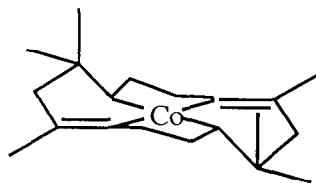
cyclam, *Trans I*



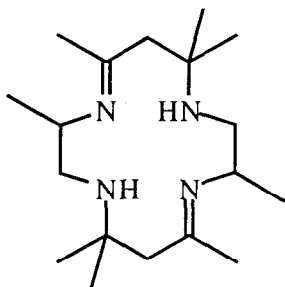
HMD



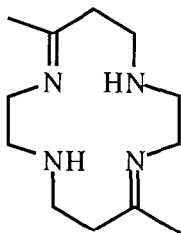
*N-rac*-HMD



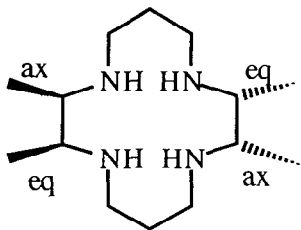
*N-meso*-HMD



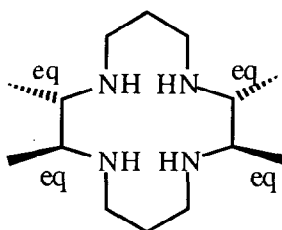
OMD



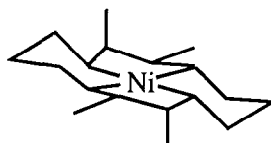
DMD



RSSR-HTIM



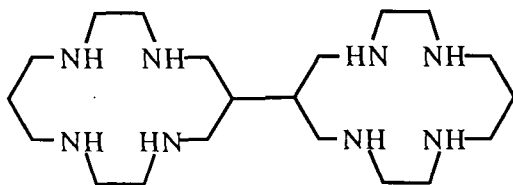
RRSS-HTIM



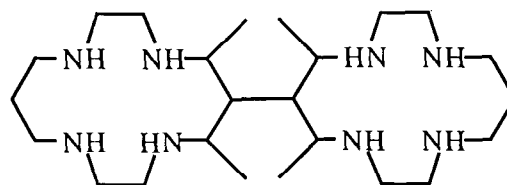
RSSR-HTIM



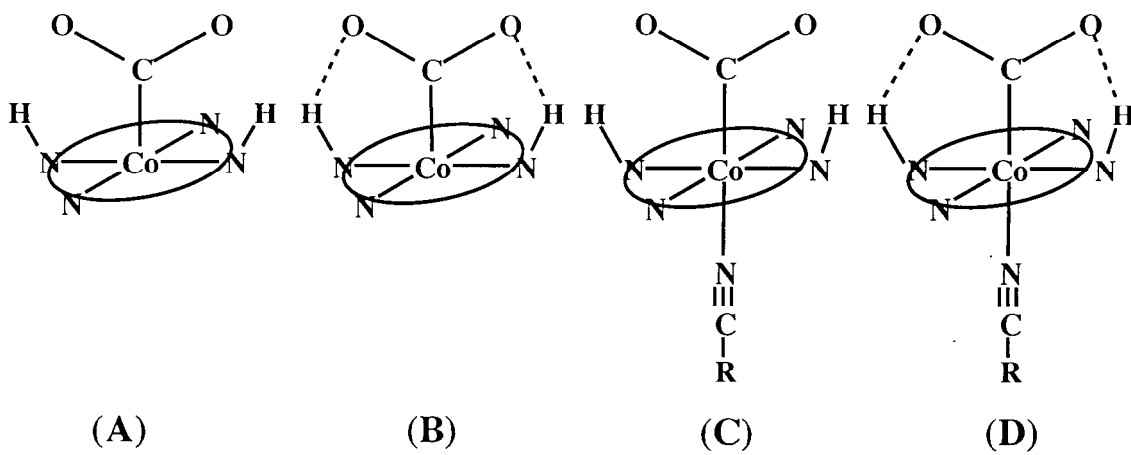
RRSS-HTIM

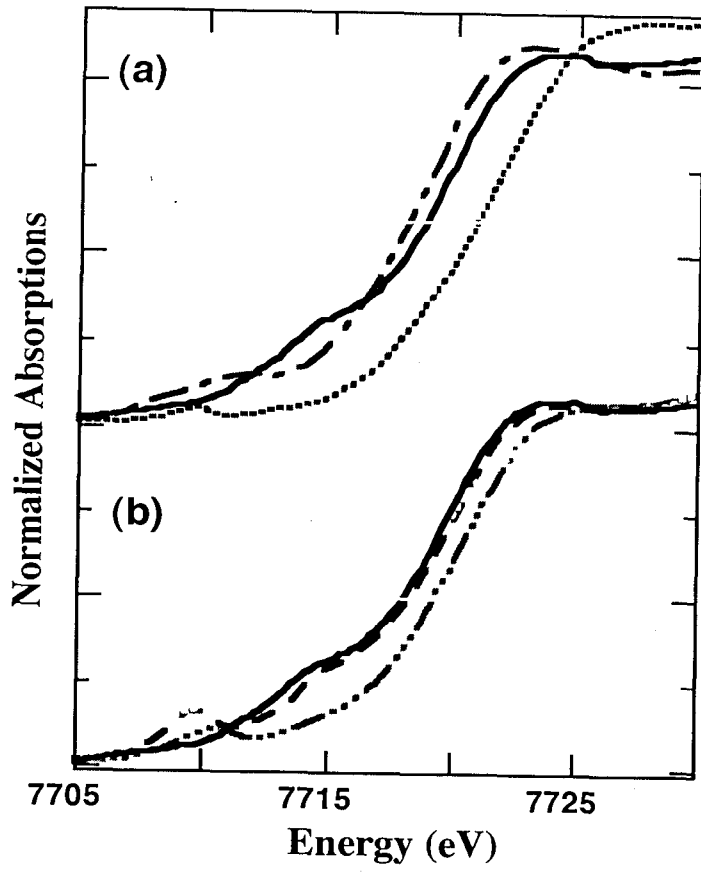


bcyclam

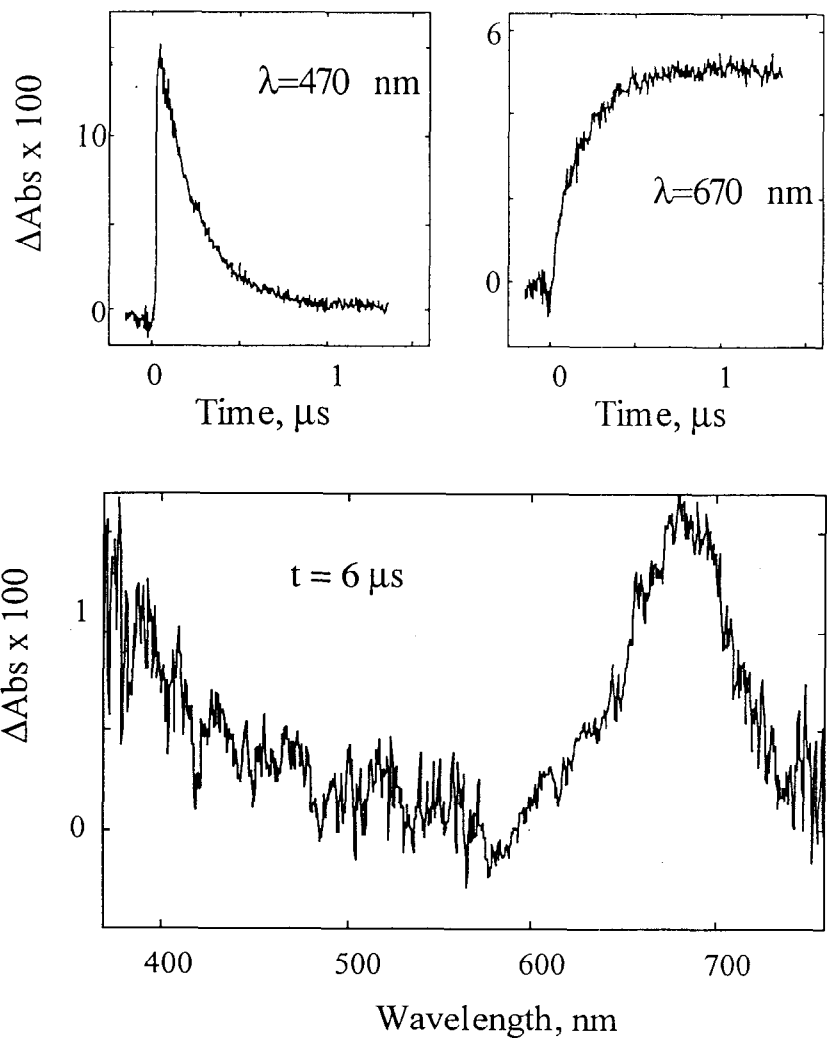


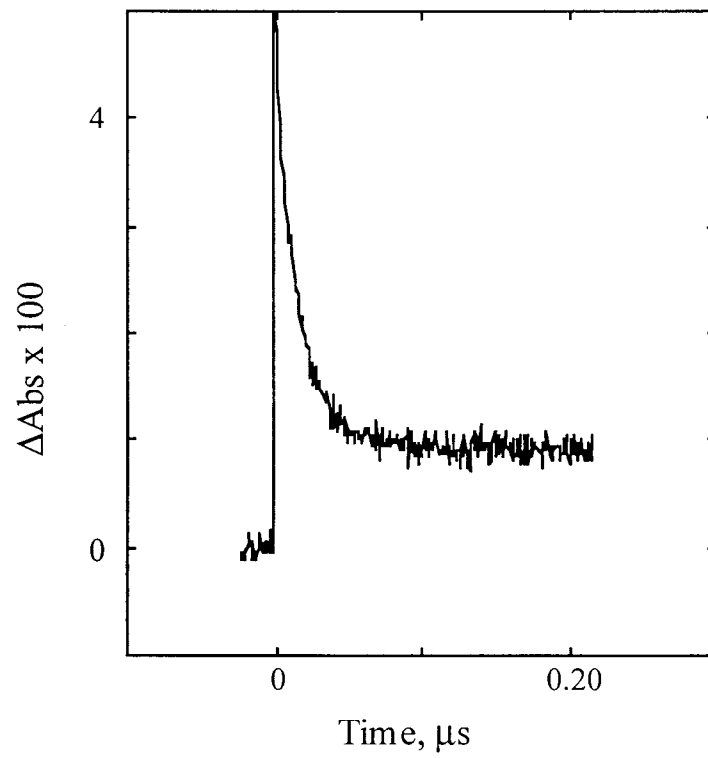
bMecyclam

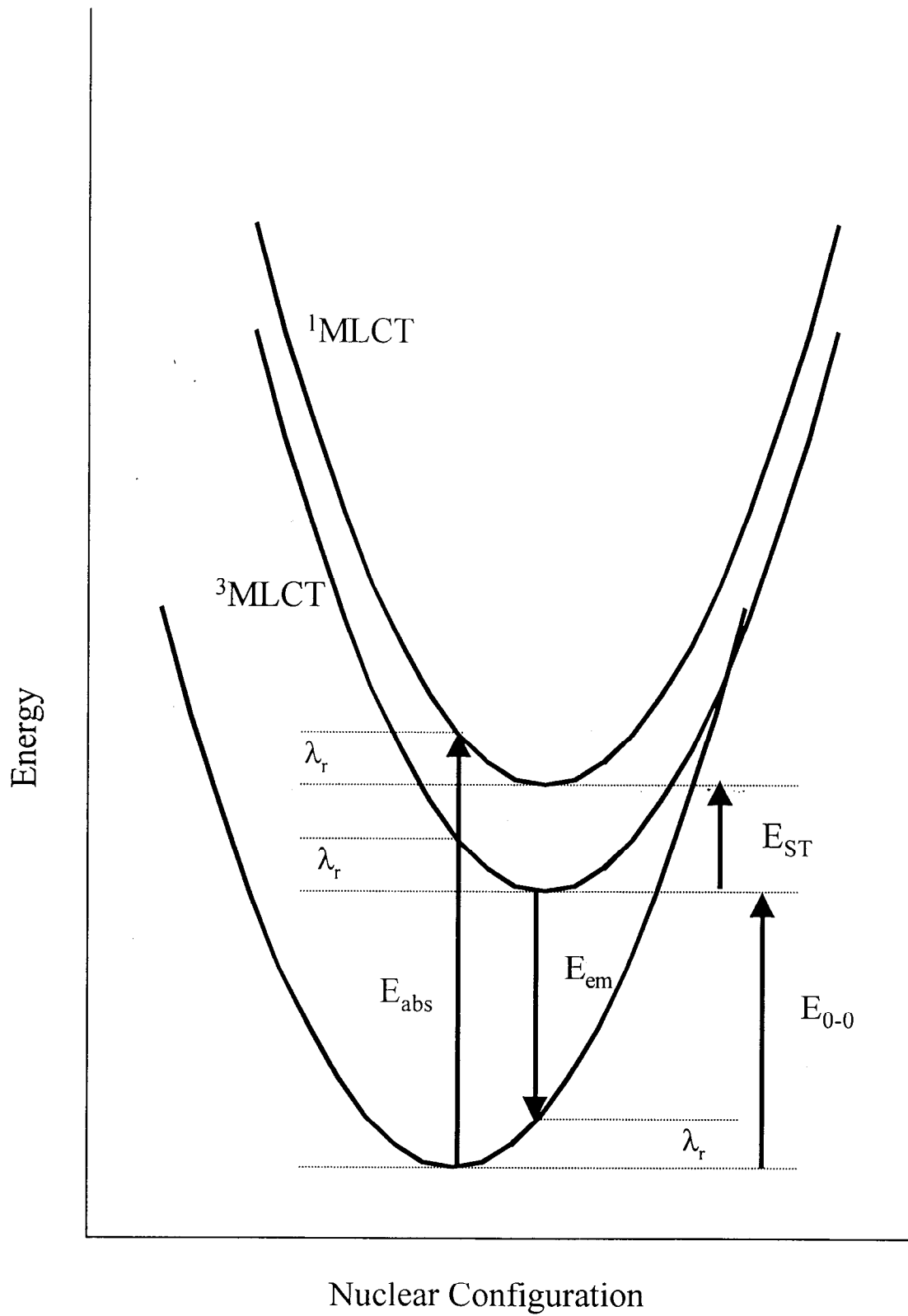


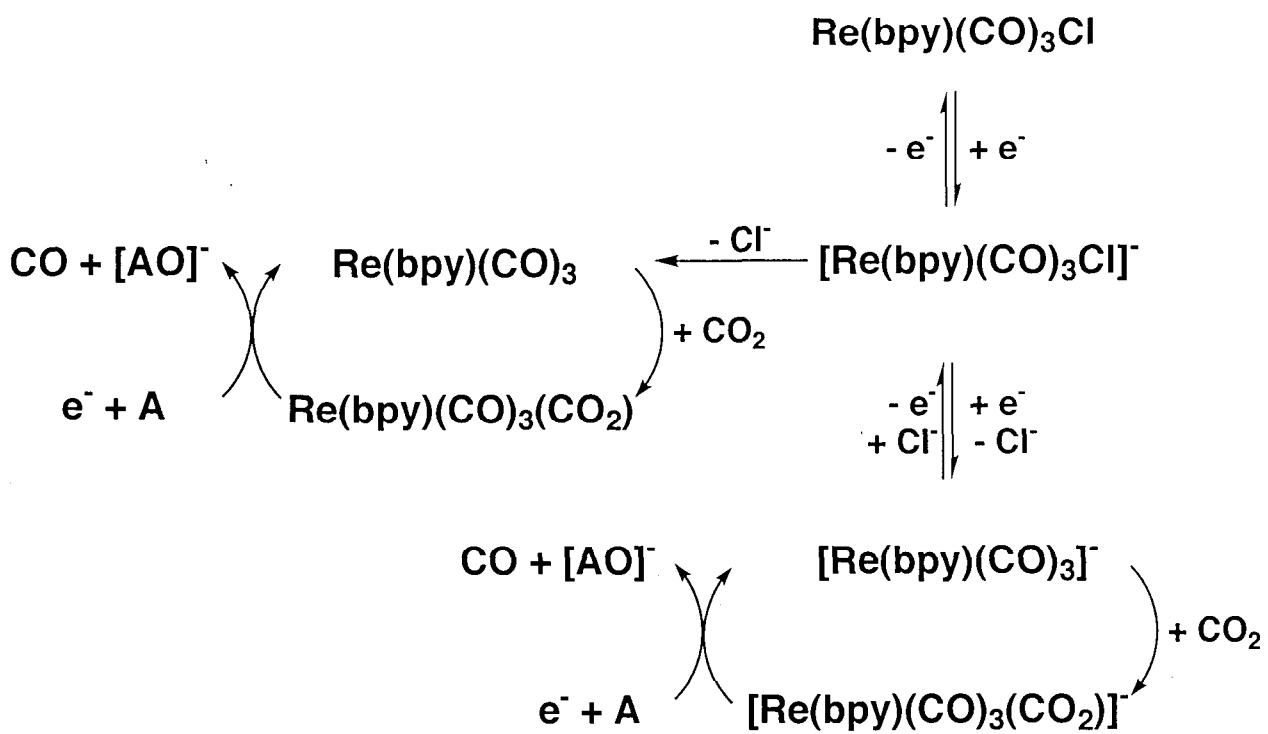


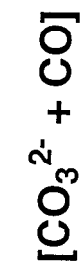
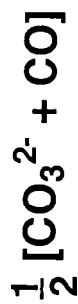




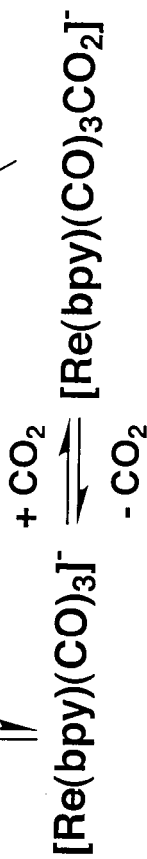
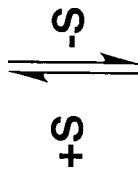
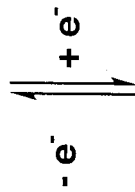








1e<sup>-</sup> pathway



2e<sup>-</sup> pathway

